



THE HONG KONG
POLYTECHNIC UNIVERSITY

香港理工大學

Pao Yue-kong Library

包玉剛圖書館

Copyright Undertaking

This thesis is protected by copyright, with all rights reserved.

By reading and using the thesis, the reader understands and agrees to the following terms:

1. The reader will abide by the rules and legal ordinances governing copyright regarding the use of the thesis.
2. The reader will use the thesis for the purpose of research or private study only and not for distribution or further reproduction or any other purpose.
3. The reader agrees to indemnify and hold the University harmless from and against any loss, damage, cost, liability or expenses arising from copyright infringement or unauthorized usage.

If you have reasons to believe that any materials in this thesis are deemed not suitable to be distributed in this form, or a copyright owner having difficulty with the material being included in our database, please contact lbsys@polyu.edu.hk providing details. The Library will look into your claim and consider taking remedial action upon receipt of the written requests.

**AIR CLEANING CONCRETE PAVING BLOCKS MADE FROM
RECYCLED CONSTRUCTION AND DEMOLITION WASTE**

ESTHER CHEUNG

A thesis submitted in partial fulfilment of the requirements for the
Degree of Master of Philosophy

The Department of Civil and Structural Engineering

The Hong Kong Polytechnic University

July 2005

I



Pao Yue-kong Library
PolyU · Hong Kong

CERTIFICATE OF ORIGINALITY

I hereby declare that this thesis is my own work and that, to the best of my knowledge and belief, it reproduces no material previously published or written nor material which has been accepted for the award of any other degree or diploma, except where due acknowledgement has been made in the text.

Esther Cheung

Abstract of thesis entitled “Air Cleaning Concrete Paving Blocks Made With Recycled Construction and Demolition Waste” submitted by Esther Cheung for the degree of Master of Philosophy at The Hong Kong Polytechnic University in February 2005.

ABSTRACT

Economic success has made Hong Kong a worldwide commercial and financial centre as well as being the gateway to China. But similar to other developed countries this path to success has put pressure on the environment. As a result air quality has suffered. The numerous tall buildings, particularly those in the urban area, hinder and prevent the dispersion of air pollutants generated by a high concentration of vehicles at the street level. It is apparent that there is a need to remove pollutants, such as nitrogen oxides (NO_x), derived from vehicular emission. Therefore, a way of removing such pollutants needs to be sought. In addition, a huge quantity of construction and demolition wastes (C&DW) is produced every day in Hong Kong, representing a large fraction of the solid waste stream. The extensive building and infrastructure development projects as well as redevelopment of old districts have led to an increase in C&DW generation in the last decade. This has caused the disposal of the wastes a severe social and environmental problem in the territory. Hence, it is necessary to find ways to overcome the growing concern of air pollution as well as the difficulty of reusing recycle aggregates.

This study aimed to analyze the effectiveness of incorporating air cleaning agents

such as titanium dioxide (TiO_2) into the concrete paving blocks which were produced by local waste materials. Factors which would affect the performance of the blocks were studied including the porosity of the blocks, the type of waste materials used within the mix design (such as recycled aggregate, furnace bottom ash and recycled glass) and the percentage of TiO_2 within the mix design. The effectiveness of different types of TiO_2 was compared.

To achieve the aim concrete blocks were produced in the laboratory and tested for their physical properties as well as their ability to remove NO. The blocks were prepared in two layers with a base layer and a surface layer. TiO_2 was only incorporated in the surface layer. The results indicated that the physical properties of the blocks were all satisfactory in meeting international standards with the compressive strength reaching 60MPa. The measurement of NO photodegradation was carried out using a reactor with the initial NO concentration of 1000ppb. The prepared specimens were placed within a sealed reactor of dimensions 700x400x130 mm and once the targeted concentration level was reached the removal of NO began when the block was irradiated by 2 UV-A lights providing an intensity of 10Wm^{-2} at the specimen surface.

Results showed that the photodegradation of NO is related to the porosity of the blocks. Generally, the higher the porosity of the block, the higher the NO removal ability. It is concluded that the choice, size and content of aggregate material used in the mix design were all important factors. In addition, crushed recycled glass was used as an aggregate in the blocks and was found to benefit the ability to remove NO due to its light transmitting characteristic. It was possible that light could be carried to a greater depth by refraction activating the TiO_2 on the surface as well as within

the blocks. Besides the type of aggregate used, the choice of TiO_2 was equally important. Three types of TiO_2 were tested in this study: (1) P-25 from Degussa Company which is a combination of anatase and rutile forms, selected due to its high purity and accurate specifications, (2) an anatase form and (3) a rutile form of TiO_2 , both sourced from Ke Xiang Company due to their low prices compared to P-25. The rutile form of TiO_2 from Ke Xiang Company showed abilities almost comparable to P-25 due to similarities in particle size. As a result an optimum mix design was selected incorporating recycled glass, sand, metakaolin, carbon and cement in the surface layer of the block and recycled aggregate and cement in the base layer of the block. The optimum mix design was used to prepare a batch of paving blocks in a factory for field testing by laying a pavement section. The air quality of the field testing site was continuously monitored to analyze the effect of the blocks towards the surrounding air quality. The observations showed that NO concentrations were reduced by 12% at ground level and 8% at breathing zone. After a period of four months the blocks were removed and taken back to the laboratory to analyze whether its ability to remove NO had decreased. Results showed only a slight decrease of 23 % for these used blocks.

ACKNOWLEDGEMENTS

I would like to thank my academic supervisor Professor C.S. Poon, for his valuable advice, support and guidance throughout the research. The objectives of the research would not have been achievable without his understanding and patience. I would also like to thank my co-supervisor Dr. S.C. Lee, for his valuable suggestions.

Thanks also given to the Civil Engineering and Development Department for supplying the recycled aggregates and to China Light Power Company Limited for supplying the furnace bottom ash and pulverised fuel ash used for this study. Appreciation is also given to the Hong Kong Correctional Services Department for assistance in manufacturing the paving blocks in the plant trial.

The financial support from the Hong Kong Polytechnic University for this project is acknowledged.

TABLE OF CONTENTS

CERTIFICATE OF ORIGINALITY	II
ABSTRACT	III
ACKNOWLEDGEMENT	VI
TABLE OF CONTENT	VII
LIST OF TABLES	<u>XII</u>
LIST OF FIGURES	<u>XV</u>

CHAPTER 1 – INTRODUCTION

1.1 Background	1
1.2 Objectives	3
1.3 Scope of works	4
1.4 Organisation of thesis	5

CHAPTER 2 – LITERATURE REVIEW

2.1 Construction and demolition waste (C&DW)	6
2.1.1 Definition	6
2.1.2 The local situation	7

2.1.3 Recycling of C&DW globally.....	9
2.1.3.1 Masonry units.....	10
2.1.3.2 Pavement sub-base.....	11
2.1.3.3 Concrete	13
2.1.4 Management and recycling of C&DW in Hong Kong.....	15
2.2 Air Pollution.....	18
2.2.1 Local problems.....	18
2.2.2 Cross border pollution.....	20
2.2.3 Pollution sources	21
2.2.4 Measures to minimise air pollution.....	25
2.3 Photocatalysis.....	26
2.3.1 Background	26
2.3.2 Common photocatalytical applications	28
2.3.3 Application of photocatalyst in construction materials.....	29
2.3.4 Titanium dioxide (TiO ₂).....	31
2.3.5 Methods of applying photocatalyst	34
2.3.6 Removal of NO using TiO ₂ photocatalysis.....	35

CHAPTER 3 – METHODOLOGY

3.1 Materials.....	38
3.1.1 Cement	38

3.1.2	Titanium dioxide (TiO ₂).....	38
3.1.3	Furnace bottom ash (FBA).....	40
3.1.4	Pulverised fly ash (PFA).....	40
3.1.5	Metakaolin (MK)	41
3.1.6	Recycled aggregates (RA)	42
3.1.7	Recycled glass (RG).....	43
3.1.8	Sand.....	43
3.2	Mix proportions.....	44
3.2.1	Mix proportions prepared with RA, FBA and sand.....	44
3.2.2	Mix proportions prepared with RG.....	48
3.2.3	Mix proportions prepared with TiO ₂	50
3.3	Sample preparation.....	54
3.3.1	Fabrication of cubes	54
3.3.2	Fabrication of surface layers	55
3.3.3	Fabrication of paving blocks.....	56
3.3.4	Fabrication of mortar bars.....	57
3.4	Determination of physical properties	59
3.4.1	Compressive strength.....	59
3.4.2	Density	60
3.4.3	Water absorption	60
3.4.4	Skid resistance.....	60

3.4.5 Abrasion	61
3.4.6 Porosity	62
3.4.7 Alkali silica reaction (ASR).....	62
3.4.8 X-ray diffraction (XRD)	62
3.4.9 Particle size distribution of TiO ₂	63
3.5 Photodegradation of NO.....	64
3.5.1 Apparatus	64
3.5.1.1 Original design	64
3.5.1.2 Revised design	66
3.5.2 Preliminary tests.....	67
3.5.3 Testing procedure.....	68
3.5.3.1 Original procedure	68
3.5.3.2 Revised procedure.....	71
3.5.4 Calculation	72

CHAPTER 4 – FACTORS AFFECTING THE NITRIC OXIDE

PHOTODEGRADATION

4.1 The effect of aggregate material on NO photodegradation.....	74
4.2 The effect of cement/aggregate ratio on NO photodegradation.....	81
4.3 The effect of curing age on NO photodegradation.....	83
4.4 The effect of particle size of aggregates on NO photodegradation.....	84

4.5 The effect of porosity on NO photodegradation 85

**CHAPTER 5 –THE EFFECT OF INCORPORATING RECYCLED
CRUSHED GLASS CULLET**

5.1 Characteristics of recycled glass in enabling NO photodegradation..... 87

5.2 Properties of recycled glass mixes 89

5.3 Enhancing NO photodegradation of paving blocks containing recycled
glass..... 91

5.4 Prevention of the paving blocks from alkali silica reaction (ASR)..... 95

**CHAPTER 6 – ENHANCING THE ABILITY OF TITANIUM DIOXIDE FOR
NITRIC OXIDE PHOTODEGRADATION**

6.1 The effect of increasing TiO₂ content of the paving blocks..... 98

6.2 Incorporating TiO₂ coated glass cullets within the mix design of paving
blocks 101

6.3 A comparison of different sources of TiO₂ 102

CHAPTER 7 – FIELD TRIAL

7.1 Mix proportions of paving blocks 108

7.2 Pilot manufacture of paving blocks..... 110

7.3 Properties of the photocatalytical paving blocks..... 112

 7.3.1 NO photodegradation 112

 7.3.2 Physical properties 113

7.4 Site trial 114

7.5 Air monitoring of paving blocks 116

7.6 NO photodegradation after field trial..... 122

CHAPTER 8 – CONCLUSIONS

8.1 Conclusions 124

8.2 Recommendations 126

REFERENCES..... 128

LIST OF TABLES

Table 2.1 Programs launched in Hong Kong to minimize air pollution [Chan <i>et al.</i> , 2001 and EPD, 2005b]	25
Table 2.2 Selected applications for photocatalysis [Fujushima <i>et al.</i> , 2000, Fujushima <i>et al.</i> , 1999 and Murata <i>et al.</i> , 1999b]	30
Table 3.1 Properties of OPC, PFA and MK.....	41
Table 3.2 Properties of TiO ₂	42
Table 3.3 Properties of RA, RG and sand.....	43
Table 3.4 Mix proportions of cubes prepared with RA and FBA.....	46
Table 3.5 Mix proportions of surface layers prepared with RA, FBA and varying TiO ₂	46
Table 3.6 Mix proportions of surface layers prepared with RA, FBA and sand.....	47
Table 3.7 Mix proportions of cubes prepared with RA, FBA and sand	48
Table 3.8 The mix proportions of cubes and surface layers prepared with RG.....	49
Table 3.9 Mix proportions of cubes and surface layers prepared with different RG.....	49
Table 3.10 Mix proportions of mortar bars and surface layers prepared with MK and PFA	50
Table 3.11 Mix proportions of cubes and surface layers with varying TiO ₂ content.....	52
Table 3.12 Mix proportions of surface layers prepared with coated glass.....	52

Table 3.13 Mix proportions of surface layers prepared with different sources of TiO ₂	53
Table 3.14 Mix proportions of surface layers prepared with varying anatase and and rutile TiO ₂ contents	53
Table 6.1 Price comparison of TiO ₂	103
Table 7.1 Mix design for surface layer	109
Table 7.2 Mix design for base layer.....	110
Table 7.3 Physical properties of the paving blocks.....	114
Table 7.4 Weather conditions for each measurement [Hong Kong Observatory, 2004]	119
Table 7.5 Data from air monitoring (P: photocatalytic paving, N: non- photocatalytic paving).....	120
Table 7.6 Percentage drop of pollutant concentration	121
Table 7.7 The activities of paving blocks	123

LIST OF FIGURES

Figure 2.1 Aggregate and rock products consumed in Hong Kong each year from 1997-2003 [Hong Kong Government, 1997-2003].....	9
Figure 2.2 Recycled paving blocks in Yuen Long [Poon, 2004]	15
Figure 2.3 Annual average of nitrogen dioxide monitoring in 2003 [EPD, 2003b]	23
Figure 2.4 Events that take place on a semiconductor in photocatalysis	27
Figure 3.1 Particle size distribution of TiO ₂ powders.....	39
Figure 3.2 XRD spectrum of TiO ₂ powders (A: Anatase, R: Rutile)	39
Figure 3.3 Cube moulds	54
Figure 3.4 Surface layer moulds	55
Figure 3.5 Paving block moulds	57
Figure 3.6 Indention mould for paving blocks.....	57
Figure 3.7 Mortar bar moulds	58
Figure 3.8 Specimen being tested for compressive strength.....	59
Figure 3.9 British pendulum skid resistance tester	61
Figure 3.10 Abrasion resistance apparatus.....	61
Figure 3.11 Bruker D8 Advance Powder Diffractometer	63
Figure 3.12 Original reactor design	65
Figure 3.13 A schematic diagram of the reactor	66
Figure 3.14 Revised reactor design.....	67

Figure 3.15 Zero air supply (Thermo Environmental Instrument Inc. Model 111)	70
Figure 3.16 Schematic diagram of the experimental set-up for the original procedure.....	70
Figure 3.17 Chemiluminescence NO analyzer (Thermo Environmental Instrument Inc. Model 42c)	71
Figure 3.18 Schematic diagram of the experimental set-up for the revised procedure.....	72
Figure 3.19 Calculation of NO removed.....	73
Figure 4.1 Compressive strength results of cubes at 28 days testing prepared with FBA and recycled fine aggregate (Table 3.4).....	75
Figure 4.2 Density measurements of cubes at 28 days testing prepared with FBA and recycled fine aggregate (Table 3.4).....	76
Figure 4.3 NO removal of specimens tested under the batch and continuous Mode (Table 3.5).....	78
Figure 4.4 Compressive strength of selected RA and sand mixes (Table 3.7)	80
Figure 4.5 Density of selected RA and sand mixes (Table 3.7).....	80
Figure 4.6 A comparison of different materials to remove NO at 90 days testing (Table 3.6).....	81
Figure 4.7 A comparison of NO removal for mixes prepared with different cement contents at 90 days testing (Table 3.6).....	82
Figure 4.8 NO removal of specimens tested at different curing ages (Table 3.6) ..	84

Figure 4.9 NO removal of specimens with different aggregate sizes (Table 3.6) ..	85
Figure 4.10 Comparison of NO removal and porosity for selected mixes.....	86
Figure 5.1 The effect of recycled glass in the mix towards NO photodegradation when compared to other materials at 90 days curing age (Table 3.6 and 3.8).....	88
Figure 5.2 The amount of acetone absorbed per 100g of dry sample for mix with recycled glass and other mixes at 90 days curing age.....	88
Figure 5.3 Compressive strength of mixes when recycled glass replaces sand as the aggregate in the mix design at 28 days curing age (Table 3.8).....	90
Figure 5.4 NO removal of mixes with different proportions of recycled glass replacing sand as the aggregate at different curing ages (Table 3.8)....	90
Figure 5.5 Compressive strength of mixes with different sources of recycled glass at 28 days curing age (Table 3.9).....	93
Figure 5.6 NO removal of mixes with different sources of recycled glass at various curing ages (Table 3.9).....	93
Figure 5.7 Possible paths of light rays for a section of a paving block prepared with recycled glass	94
Figure 5.8 Possible paths of light rays for a section of a paving block prepared with recycled fine aggregates.....	94
Figure 5.9 Expansion of mortar bars with MK addition by cement weight at 2.5%, 5% and 10% (Table 3.10).....	96

Figure 5.10 Expansion of mortar bars with PFA addition by cement weight at 2.5%, 5% and 10% (Table 3.10).....	96
Figure 5.11 NO removal of mixes with either MK or PFA addition by cement weight at 0%, 2.5%, 5% and 10% (Table 3.10)	97
Figure 6.1 The effect of compressive strength with increasing TiO ₂ content (Table 3.11).....	99
Figure 6.2 The effect of density with increasing TiO ₂ content (Table 3.11)	100
Figure 6.3 The effect of NO removal at different TiO ₂ contents (Table 3.11)	100
Figure 6.4 NO removal of specimens with and without TiO ₂ coated glass cullets (Table 3.12).....	102
Figure 6.5 NO removal of specimens containing different sources of TiO ₂ (Table 3.13).....	104
Figure 6.6 NO removal at different TiO ₂ (anatase) contents (Table 3.14)	106
Figure 6.7 NO removal at different TiO ₂ (rutile) contents (Table 3.14).....	107
Figure 7.1 Materials poured into mixer chute	111
Figure 7.2 Machinery	111
Figure 7.3 Block manufacture.....	111
Figure 7.4 The final products	111
Figure 7.5 NO removal of B-1, B-2 and B-3 and different curing ages (Table 7.1 and 7.2).....	113
Figure 7.6 Distant view of site location	115

Figure 7.7 Photocatalytic pavement.....	115
Figure 7.8 Close-up of photocatalytic pavement and original pavement.....	115
Figure 7.9 Map of site location [Centamap, 2004]	116
Figure 7.10 Sampling locations.....	118
Figure 7.11 Collection of air bag at breathing zone.....	118
Figure 7.12 Commercially available photocatalytic block	123
Figure 7.13 Self-designed photocatalytic block.....	123

1. Introduction

1.1 Background

The construction industry is the major solid waste generator in Hong Kong [Poon, 2001b]. The extensive building and infrastructure development projects as well as redevelopment of old districts have led to an increase in construction and demolition waste (C&DW) generation in the last decade. This has caused the disposal of the wastes to become a severe social and environmental problem in the territory. Up to present this problem has been dealt with by disposing the waste at landfills and public filling areas locally. There is an increasing interest to explore new ways to recycle aggregates derived from C&D waste [Fong, 2003].

Additionally Hong Kong also faces the growing concern of air pollution due to having to provide habitats and transportation for a high population density of seven million people [Chan *et al.*, 2001]. The numerous tall buildings, particularly in the urban area, hinder and prevent the dispersion of air pollutants generated by a high concentration of vehicles at the street level. It is apparent that there is a need to remove pollutants, such as nitrogen oxides (NO_x) and sulphur dioxide (SO₂) from the atmosphere. Not only do these gases pose a threat to health, they are also causing degradation to many inner city buildings. Despite attempts to lower these emissions

by using cleaner vehicles, it appears that a way of removing such pollutants once in the atmosphere needs to be sought.

Photocatalysis, such as titanium dioxide, have already been tested in Japan for concrete paving materials that can facilitate a photocatalytic reaction converting the more toxic forms of air pollutants to less toxic forms (e.g. NO_x to HNO₃) [Anpo, 2003, Murata, 1999a, Murata, 2002, Okura and Kaneko, 2002]. Under the illumination of ultraviolet light, photocatalysis shows diverse functions, such as the decomposition of air and water contaminants and deodorization, as well as self cleaning, antifogging, and antibacterial actions [Aoki, 2002, Fujushima *et al.*, 1999, Fujushima *et al.*, 2000, Murata, 1999b]. The term photocatalysis combines photochemistry and catalysis, and implies that light and a catalyst are required to accelerate a chemical transformation. Practical applications of photocatalysts have rapidly expanded in recent years. Photocatalytic materials for outdoor purification are in urgent demand because energy and labour saving advantages have been realized when applied to building or road construction materials in large cities where urban air pollution is very serious [Murata, 1999b].

1.2 Objectives

Based on the current environmental problems the main objective of this project was to analyze the effectiveness of incorporating air cleaning agents such as titanium dioxide (TiO_2) into the technique of producing concrete paving blocks using local waste materials.

Factors which would affect the performance of the blocks were considered and as a result the following additional objectives were identified:

- Investigate the durability of the paving blocks when used for construction purposes and also the effectiveness towards pollutant removal, by using suitable methods.
- Derive a suitable and optimum mix proportion for the paving blocks, which would be responsible for air pollutant abatement purposes.
- Compare natural aggregates with recycled aggregates and decide which benefits the pollutant removal ability of the paving blocks.
- Study the factors affecting the NO photodegradation of the blocks. These include porosity, cement content, different particle size of aggregates, curing age and derive an optimum mix proportion considering these factors.
- Investigate whether recycled glass is beneficial to the mix design of paving blocks, resulting in better pollutant removal ability.
- Compare different sources of TiO_2 and the effects towards pollutant removal ability.

1.3 Scope of works

The following tasks were carried out in order to fulfill the objectives of this project:

- The proposed research commenced with a literature review, followed by an experimental programme preparation.
- Paving blocks were prepared with a concrete base layer made from cement and recycled aggregates, and a thin surface layer made of cement, recycled materials, and a small amount of titanium dioxide. The physical and mechanical properties were identified and suitable mixes for the photocatalytic blocks were selected.
- Surface layers were produced using different materials and combinations, and tested for their ability to remove pollutants.
- For selected optimal mixes, plant trial was conducted with a local block manufacturer.
- The durability properties of the blocks after exposure to polluted air were assessed.

1.4 Organisation of thesis

This thesis is divided into eight chapters. The present chapter covers the background, objectives and scope of this project. A brief literature review is given in Chapter two. Chapter three contains detail of the materials and methods used in this project.

The analytical results obtained are presented and discussed in Chapters four to seven. Chapter four focuses on the factors affecting the NO photodegradation of the prepared surface layers. Chapter five concentrates on the effect of incorporating recycled crushed glass cullet into the mix design of the surface layer. Chapter six analyses the methods used to enhance the ability of TiO₂ for NO photodegradation. Chapter seven looks at the manufacturing process of the optimum mix design and the results from field testing. Chapter eight reviews the major findings of this project with recommendations included.

2. Literature review

2.1 Construction and demolition waste (C&DW)

2.1.1 Definition

C&DW is defined by the Hong Kong Environmental Protection Department [EPD, 2003a] as:

C&D material is a mixture of surplus materials arising from site clearance, excavation, construction, refurbishment, renovation, demolition and road works. Over 80 % of C&D material are inert and are known as public fill. Public fill includes debris, rubble, earth and concrete which is suitable for land reclamation and site formation. When properly sorted, materials such as concrete and asphalt can be recycled for use in construction. The remaining non-inert substances in C&D material are called C&D waste which includes bamboo, timber, vegetation, packaging waste and other organic materials. In contrast to public fill, C&D waste is not suitable for land reclamation and is disposed of at landfills.

2.1.2 The local situation

Up until 2003 the construction industry has been the major solid waste generator in Hong Kong. The extensive building and infrastructure development projects as well as redevelopment of old districts have led to an increase in C&DW generation in the last decade. This has caused the disposal of the wastes to become a severe social and environmental problem in the territory. Up to present this problem has often been dealt with by disposing of at landfills and public filling areas locally.

According to the Hong Kong Civil Engineering Development Department in 2003 [CEDD, 2003] 19.6 million tonnes of C&D materials was generated. Of this amount, over 80 % (17.10 million tonnes) were inert materials. The remaining proportion represented less than 20 % (2.50 million tonnes) of the total C&D materials generated in 2003, these were non-inert materials. C&DW has been taking up valuable landfill space, on this trend Hong Kong landfill space will run out within 7 to 11 years [EPD, 2004].

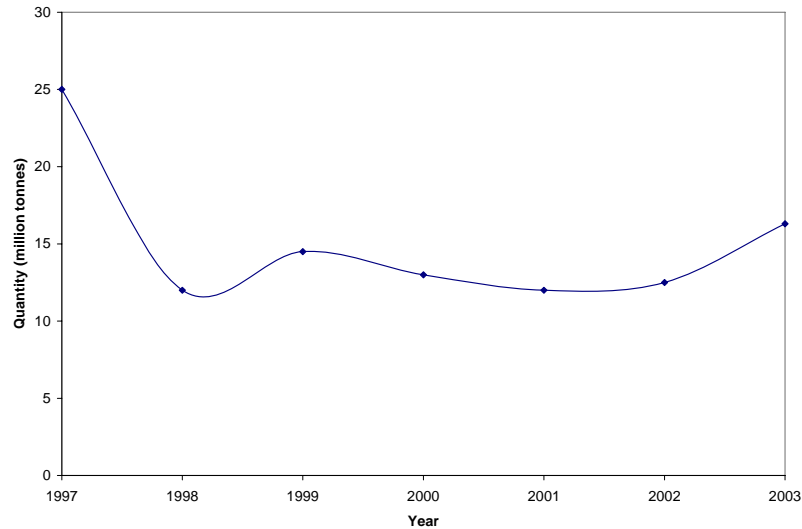
Hong Kong is also running out of public filling areas, which has traditionally been used to accommodate the large amount of inert granular materials generated from excavation & demolition. In recent years, public concerns and objections have often delayed, reduced the scale of or stopped the implementation of planned reclamation projects (particularly those within the Victoria Harbour). As a result there will be no

further new reclamation projects. Hence the shortage problem for landfill space will be aggravated.

The existing large quantities of C&DW together with the continuous increase has drawn environmental awareness from the society and has meant that there has been pressure to recycle.

To recycle C&DW as recycled aggregates for construction could benefit the local economy. Figure 2.1 shows the quantity of aggregates and rock products consumed in Hong Kong each year from 1997-2003. Presently 40 % of the aggregate demand in Hong Kong has to be imported from southern China due to the local deficiency [Chan and Fong, 2001]. The remaining 60 % is achieved locally, but if recycled aggregates can be produced from local C&DW, they can act as a substitute for virgin aggregates to meet the necessary demand.

Figure 2.1 Aggregates and rock products consumed in Hong Kong each year from 1997-2003 [Hong Kong Government, 1997-2003]



2.1.3 Recycling of C&DW globally

In Europe the recycling of building materials started towards the end of World War II when bricks and other materials recovered from the ruins of war, were utilized for reconstruction of amenities [Olorunsogo, 1999]. Similarly inert materials from C&DW can be sorted and crushed to provide recycled aggregates for construction applications. The high quality of recycled aggregate produced has meant that countries in Europe, Japan and United States have all modified their specifications to adapt with the growing trend of using recycled aggregate in construction works. The use of recycled aggregate has been extensively studied in road construction for sub-base [Cuperus and Boone, 2003]. More recent applications for recycled aggregate

include the production of Portland cement concrete and masonry units. Recycled aggregate is often used for road sub-bases and masonry units instead of concrete as the requirements for these tend to be less strict and also because more research has been carried out to prove the ability for these applications. The use of recycled aggregate for masonry units, pavement sub-bases and concrete are further investigated in this chapter.

2.1.3.1 Masonry units

The use of recycled aggregates to produce masonry products is still relatively new. An early attempt was made by Collins *et al.* [1998] who used recycled aggregates in the manufacture of blocks for a beam-and-block floor system. The blocks were 440 mm long, 215 mm wide and 100 mm high. Recycled aggregates were used to substitute 25 to 75 % by weight of both natural coarse and fine aggregates. For blocks with a replacement level of 75 %, a compressive strength of 6.75 MPa and a transverse strength of 1.23 MPa were reported.

Subsequently Poon *et al.* [2002] successfully designed a patented technology in using a mechanized moulding method for producing concrete bricks and paving blocks. The method can replace both the fine and coarse natural aggregates by local recycled aggregates in making the precast products. Using this technique, concrete paving blocks complying with the requirements of the General Specifications

[CEDD, 1992] with a compressive strength of not less than 30 MPa can be produced.

The recent developments have showed obvious advantages and proved that recycling C&DW and reusing as recycled aggregate in masonry units is feasible. Products including partitioning walls, road dividers, bridge fencing, noise barriers and paving blocks can be produced, all of which do not require high quality standards.

2.1.3.2 Pavement sub-base

Pavement is a multi-layers structure, typically composed of either a concrete or an asphalt slab resting on a foundation system. The foundation system consists of various layers such as the base, sub-base, and sub-grade. Conventionally, natural materials such as crushed rocks, selected gravels and stabilized materials are used in road bases. Over the last two decades, research has been undertaken to investigate the possibility of using recycled aggregate in road bases in order to provide a viable option for the use of recycled aggregate.

Chini *et al.* [2001] tested the properties of a road base sample using recycled aggregate produced from a demolished concrete pavement which had a design mix strength of 20 MPa. The sample was tested for gradation, lime rock bearing ratio

(LBR), LA abrasion and soundness loss in accordance with AASHTO T 27-93, FM 5-515, AASHTO 96-94 and AASHTO T 104-94, respectively. Test results showed that the road base sample passed all standard requirements of gradation, LBR and LA abrasion with the exception of the soundness test using sodium sulfate. In addition they claimed that the mortar adhered to the recycled aggregate was reactive to sodium sulfate and contributed to an increased loss in the soundness test.

Park [2003] tested the physical and compaction properties of two different recycled aggregates obtained from a housing redevelopment site (RCA-1) and a concrete pavement rehabilitation project (RCA-2). The bulk specific gravity and water absorption values were 2.527 and 2.539 and 1.43 and 1.77 % for RCA-1 and RCA-2, respectively. The optimum moisture contents were 9 % and 12.8 % and the corresponding dry densities were 2.21 and 1.81 Mg/m³ for RCA-1 and RCA-2, respectively. It was apparent that optimum moisture content increased with an increase in water absorption of the aggregates.

Nataatmadja and Tan [2001] tested the resilient response of a sub-base material made with four different recycled aggregates. The aggregates were originated from concretes with compressive strengths of 15, 18.5, 49 and 75 MPa. The corresponding ten percent fines values were 149, 158, 166 and 187 for the four different recycled aggregates respectively where the ten percent fines values increased with increasing compressive strength of the original concrete. The resilient response of a sub-base material made with recycled aggregate was found to

be comparable to that of a sub-base material made with natural aggregate and also to be dependent on the strength of the original concrete, the amount of softer material in the recycled aggregate and the flakiness index.

2.1.3.3 Concrete

Slump, a workability measure, was found less for concrete containing recycled aggregate [Rashwan and Abourisk, 1997 and Dhir *et al.*, 1999]. This phenomenon is mainly attributed to the physical properties of the recycled aggregate's shape and texture and water absorption. The angularity and the rough texture of recycled aggregate create higher internal friction, thus increasing the shear strength capability of concrete and reducing the slump. Recycled aggregate is generally more porous than natural aggregate. Owing to this reason, concrete with recycled aggregate absorbs a higher amount of water than that of conventional concrete. The high water absorption by recycled aggregate can be mitigated by pre-wetting or by partly saturating the aggregate prior to mixing. Although increasing the water content can improve the workability of concrete, it is not recommended since the strength and durability of the resulting concrete will be adversely affected. Nevertheless, if water content is increased, cement content has to be increased accordingly in order to maintain the same water to cement ratio. An alternative way to improve workability of recycled aggregate concrete is to use a super plasticizer. Super plasticizers can disperse the flocculated cement grains, thus improving the workability of concrete.

Experiments conducted by various researchers also revealed that recycled aggregate concrete has a higher air content and a lower density compared to concrete made with natural aggregate [Rashwan and Abourisk, 1997 and ECCO, 1999].

The compressive strength of recycled aggregate concrete is generally 5 to 10 % lower than concrete made with natural aggregate when the same water-to-cement ratio is used [ECCO, 1999]. Studies carried out by Chen *et al.* [2003] showed drops from 15 to 25% for recycled aggregate concrete with different brick and tile content in the recycled aggregate.

Experiments conducted by various researchers show that the tensile strength is marginally affected by the use of recycled aggregate derived from both concrete and masonry [Khaloo, 1994, Tavakoli and Soroushian, 1996 and Ryu, 2002]. Zakaria [1999] reported that concrete with crushed brick as coarse aggregate has a tensile strength slightly higher than that of natural aggregate concrete.

The modulus of elasticity is reduced if recycled aggregate is used. The reduction ranges from 15 % to 40 % [ECCO, 1999]. Similarly, Mansur *et al.* [1999] evaluated the effect of using crushed brick as coarse aggregate on the modulus of elasticity of concrete. They found that concrete using crushed brick, regardless of the water to cement ratio, generally had a modulus of elasticity value, which was approximately 23 percent lower than that of conventional concrete.

2.1.4 Management and recycling of C&DW in Hong Kong

Recycling as a means of sustainable use of materials started in Asia until fairly recently. The progress of recycling of C&D materials is relatively slower in Hong Kong. The major constraint is the lack of knowledge about recycled aggregate (especially in concrete) within the construction industry in Hong Kong. The current problems in landfill and public fill shortage have led to the development of environmentally friendly alternatives.

Poon [2004], demonstrated the practical use of paving blocks made using recycled aggregates. The paving blocks were manufactured, paved and monitored locally. Figure 2.2 shows one of these sites in Yuen Long which has been laid for almost two years. The study demonstrated that both fine and coarse aggregates could be used to replace virgin aggregates in concrete paving blocks of grade 30.

Figure 2.2 Recycled paving blocks in Yuen Long [Poon, 2004]



In order to initiate the establishment of the recycling market the government set up the first temporary recycling facility in 2002 within a public filling area in Tuen Mun Area 38, to process inert C&DW into aggregate products for use in public projects, research and development works in Hong Kong. The plant was designed to cope with a handling capacity of 2400 tonnes of recycled aggregates per day and a designed output capacity of 1200 tonnes of recycled aggregates per day [CEDD, 2004a]. The plant produces recycled coarse aggregates (40, 20 and 10 mm), recycled fine aggregates (<5 mm) and recycled rock fill (grade 20). Over two and a half years the plant has produced 441,963 tonnes of recycled aggregate for beneficial reuse in construction works [CEDD, 2004b].

The government has also been planning to establish a medium term recycling facility at Kai Tak to maintain the continuous supply of recycled aggregate after the decommissioning of the facility in Tuen Mun 38. A site of 4.7 ha. has been reserved for the plant located within the middle section of the old runway. The land will be let out for short term tenancy of approximately 5 years. The recycling facility will have a capacity to handle 4000 tonnes of C&DW a day [CEDD, 2004c].

Since 2003 the local government has required all public work tenders to submit waste management plans for construction site projects [CEDD, 2003]. The plan acts as a guideline for the tenders to handle their C&DW wisely, by sorting the waste at source (on-site) to enable efficient reuse and recycle. The enforcement of waste

management plans for public works additionally aim to encourage the public sectors to follow.

In 2002 two local fill banks were built to act as a temporary storage for inert C&DW for future use. In the meantime surplus good quality rock is redirected from public fills to be processed into rock products for use in asphalt and concrete production [CEDD, 2003].

Another recent step forward is that a charging scheme for C&DW disposal has been implemented [EPD, 2004]. The scheme details that inert waste going to public fills should be charged at HK\$27/tonne. Mixed waste going to sorting facilities with at least half comprising inert waste should be charged at HK\$100/tonne. And mixed waste going to landfills with less than half comprising of inert waste should be charged at HK\$125/tonne.

The wetland park in Tin Shui Wai has also successfully utilized recycled aggregate concrete [HKWLP, 2004]. Continuous studies involving the use of recycled aggregate include trials carried out by the Hong Kong Polytechnic University for the use of RA for sub-base.

2.2 Air pollution

2.2.1 Local problems

Air pollution is any material that is introduced into the air in such quantities that it creates a significant local, regional, or global health, welfare, or ecological impact [Palmgren *et al.*, 1996]. Hong Kong faces similar serious air pollution problems as other major international cities such as Los Angeles, Mexico City, Tokyo and London.

Air quality in Hong Kong coincides with specific conditions of climate and geography. During windy seasons, pollutants can easily be removed at a high rate. But the removal becomes less efficient when pollutants are trapped amongst tall buildings. Heated by sunlight, polluted air rises and mixes with clean air in the upper atmosphere, which efficiently dilutes pollutants suspended in the air.

But Hong Kong's high population density and geographical features have an adverse effect on air circulation, making it difficult for polluted air to disperse. The result is that the climate's natural mechanism for removing pollutants can no longer minimize the impacts of air pollution effectively. Natural movement of wind has trouble dispersing such trapped fumes due to tall buildings.

Common to all developing regions of the world where economic factors outweigh environmental concerns, Hong Kong became a severely polluted city during the 1970s when the manufacturing industries flourished together with an expansion in population and rapid urban development. It was only until 1981 that control legislation was put in force and Hong Kong's Environmental Protection Department (EPD) was established to tackle the situation [Wong and Tanner, 1997].

Rapid urbanization, infrastructure construction and even commercial activities can affect the local climate. Temperatures rising in urban areas such as Hong Kong can be referred to as the 'heat island effect', which is caused by high frequencies of economic activities trapping fine particulates and reducing visibility [Chan *et al.*, 2001].

Pollution from industry and power plants was the main concern in the 1970s and 1980s, but as businessmen became aware of the cheap labour and low running costs in south China these were moved northwards. This hence brought vehicle pollution to the forefront in the 1990s. Emissions from road transport tend to account for a higher proportion of the total emission in urban areas. For example in 1995 emissions of NO_x in London from road transport were estimated to be responsible for 75% of total emissions [Devahasdin *et al.*, 2003]. Hong Kong is now believed to have the highest density of vehicles in the world of 271 vehicles per km of road space compared to in the United States where there are only 33 vehicles per km road space [Hung *et al.*, 2002]. Air pollution indices published by the authority in Hong

Kong indicate pedestrians may suffer severe health risk associated with the poor air quality in the congested urban roads and streets. Pollutants discharged from automobiles particularly diesel motorcars remains a problem.

2.2.2 Cross border pollution

Another source of major road traffic pollution in Hong Kong is cross border transport. The number of vehicles in China tripled from 1984 to 1994 and by the year 2020 the urban vehicle population is expected to be 13 to 22 times greater than it is today [Chan *et al.*, 2001]. With the growth of business between south China and Hong Kong during the 1990s, cross border traffic has increased tremendously in the past decade. More than 90% of the vehicles crossing the border are heavy diesel vehicles, generally poorly maintained and frequently overloaded. In addition, due to economic reasons low grade diesel fuel from the mainland is used by most of these vehicles increasing emissions. These problems accelerate the pollution problem in Hong Kong especially around the border area.

Part of Hong Kong's air quality problem appears to be associated with the large scale and extensive urbanization and industrialization that have occurred in the neighbouring Guandong Province. This was a result of the relocation of the manufacturing industry away from Hong Kong during the 1980s and 1990s, and the continuing investment by Hong Kong entrepreneurs in the province's industries, housing and infrastructure.

Local and regional effects of pollution are not solely caused by local emission sources as some pollutants might have blown in by the strong prevailing winds from Mainland China [Texas A&M University, 2001].

China's rapid economic growth and under developed pollution control measures, together with the increasing number of vehicles is believed to be tied to Hong Kong's ability to lower pollutant levels. Hence the Hong Kong government is aware that air pollution prevention needs to be carried out with the cooperation of our neighbouring province.

2.2.3 Pollution sources

Due to the increase in harmful emission gases in the World's inner cities, it is apparent that there is a need to remove pollutants. Not only do these gases pose a threat to health, they are also causing degradation to many inner city buildings [Dalton *et al.*, 2002]. Despite attempts to lower these emissions from cars, it appears that a way of removing such pollutants once in the atmosphere needs to be sought.

Pollution of the atmosphere increases in almost direct ratio to the population density and is largely related to the products of combustion from heating plants, incinerators, and automobiles, plus gases, fumes, and smokes arising from industrial processes [Sawyer *et al.*, 2003].

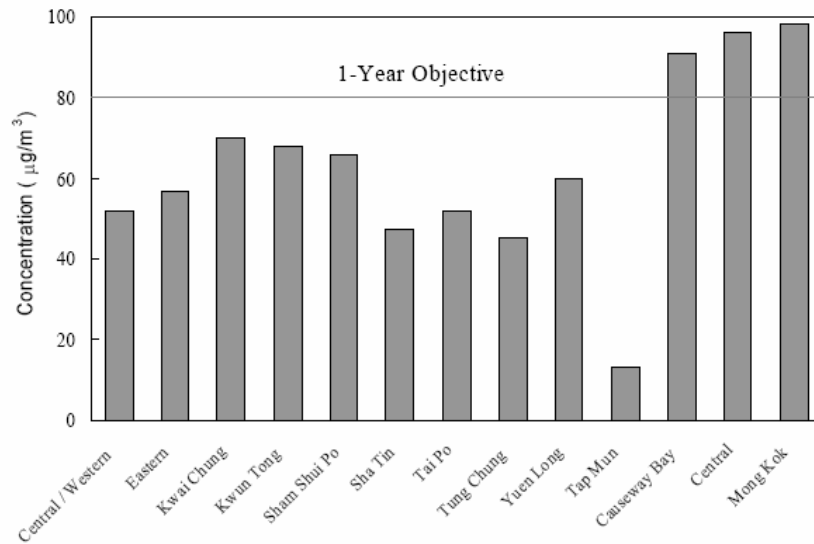
In order to tackle the problems the local EPD carries out a lot of data collection work for air quality management, research and to analyze the effectiveness of current air pollution control programs. A network of 14 air quality monitoring stations to measure major air pollutants are set up around Hong Kong, 11 to monitor general air quality and 3 to monitor roadside air quality (Causeway Bay, Central and Mong Kok). The monitoring of roadside quality is internationally rare but much of Hong Kong's air pollution arises from the congested traffic hence the three monitoring stations are set up in areas with high volumes of vehicles.

Increasingly, governments around the world are setting air pollution standards to protect both human health and the wider environment. But in Hong Kong there are no such standards instead the government propose Air Quality Objectives (AQO) which are not compulsory by law.

The level of air quality is often referred to as the Air Pollution Index (API) which is calculated by comparing the measured concentrations of pollutants with their respective health related AQO. API ranges from 0 to 500 according to their potential effects to health, if the index exceeds 100 short term AQO health warnings are issued. Among the seven atmospheric pollutants for which the air quality objectives are set by the authorities, ozone, particulate matter and nitrogen oxides are the main contributors to high API readings in Hong Kong [Civic Exchange, 2004a].

Since 1999 the EPD were aware of the seriousness of roadside air pollution hence monitoring began especially in heavy traffic areas. The concern for air quality was correct as both particulate matter and nitrogen dioxide exceeded the long term 1 year AQO (Figure 2.3).

Figure 2.3 Annual average of nitrogen dioxide monitoring in 2003 [EPD, 2003b]



Nitrogen oxides (NO_x) which consist of 85-97% nitric oxide (NO) and the rest nitrogen dioxide (NO₂), represent a larger fraction of the vehicular emissions in Hong Kong than they do in most other industrialized cities. The Hong Kong EPD reported on their website that vehicles contributed about 75 % of the NO_x in Hong Kong [EPD, 2005a]. This is again due to the composition of the vehicle fleet and the reliance on low grade diesel in the past. The emission of NO_x from road traffic is typically less than 50% of the total emission but because the emission from vehicles occurs near the ground in contrast to the emission from power plants and

industries the road traffic attributes up to 90% of the concentration in urban air [Palmgren *et al.*, 1996]. NO_x is responsible for tropospheric ozone/particulate (urban smog) through photochemical reactions with hydrocarbon. Further, NO_x together with SO_x (sulfur dioxide and sulfur trioxide) is the major contributor to the "acid rain" that harms forest and crops, as well as aquatic life [Devahasdin *et al.*, 2003]. This pollutant is also known to cause a wide range of environmental damage, including visibility impairment and eutrophication.

NO₂ is mainly formed from the oxidation of NO emitted from fuel combustion. Power station (45%) and motor vehicles particularly diesel vehicles (31%) are the two major sources of NO₂ in Hong Kong [Civic Exchange, 2004b]. NO₂ emissions from motor vehicles are of great concern due to their direct influence on the roadside air quality. It is also believed to be the most serious air pollutant on the roadside which often exceeds the value stipulated by the Hong Kong Air Objectives as indicated by roadside monitoring results [Lam *et al.*, 1999]. Long-term exposures to NO₂ can lower a person's resistance to respiratory infections, irritation and aggravate existing chronic respiratory diseases. Short-term exposure may cause increased respiratory illness in young children and harm lung function in people with existing respiratory illnesses.

2.2.4 Measures to minimise air pollution

To tackle the severe air pollution problem, the Hong Kong government has launched a series of programs aimed to reduce particulate emissions from motor vehicles by 80% and nitrogen oxide emissions by 30% before 2005. Table 2.1 describes some of these programs.

Table 2.1 Programs launched in Hong Kong to minimize air pollution [Chan *et al.*, 2001 and EPD, 2005b]

Program	Detail
Adopt tighter fuel and vehicle emission standards	The Euro III emission standards have been implemented in step with the European Union. Diesel vehicles that comply with the standards produce 40% less nitrogen oxides than a pre-Euro vehicle manufactured 6 years ago.
Adopt cleaner alternatives to diesel where practicable	Better air quality can be achieved by adapting alternative types of fuel. Electric vehicles are considered as the cleanest alternative producing zero emission. Other types of environmentally friendly fuel include liquefied petroleum gas (LPG) and low sulphur fuel, which have both been successfully applied in Hong Kong. In addition every diesel taxi replaced by one that operates on LPG is subsidized, the aim of this move is to encourage a quick switch from diesel to cleaner fuel.
Strengthening emission inspection and enforcement	The EPD operates a smoky vehicle emission control program that requires smoky vehicles spotted by accredited spotters to undergo a smoke test within a specified period. Failure to pass the test will result in the vehicle license being cancelled.
Environmental education	The Government kicked off a campaign in September 2001 to promote "switching off engines while waiting". Guidelines have been issued to the transport trade on this good practice.

2.3 Photocatalysis

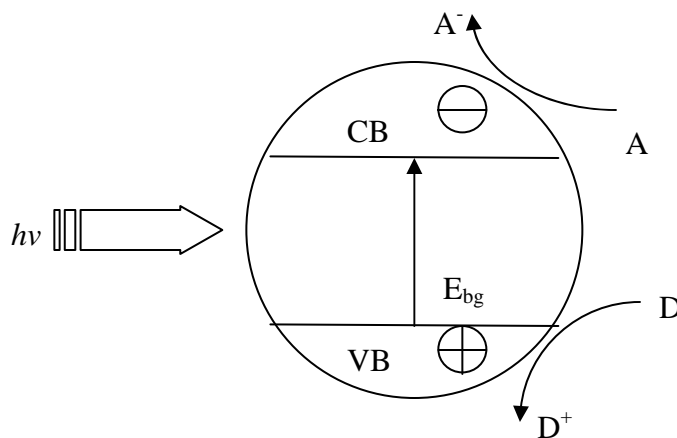
2.3.1 Background

The term photocatalysis was first introduced into the glossary of science in the early 1930s [Parmon, 1997]. Initially photocatalysis was not defined accurately as there was little research and information related. The knowledge in this area related to biogenic forms of photocatalysis such as in natural photosynthesis of plants, it was only known that solar energy was required for chemical conversions. It was only until 1972 Fujishima and Honda discovered that water could be split by illuminating TiO_2 electrodes. Their discovery was one of the first attempts in photoinduced redox reactions and drew the attention of other scientists and researchers to investigate further. The advantages of photocatalysis have meant that its use has been extensively researched but over the past decade environmental awareness has drawn more attention to the usage of photocatalysis for environmental applications [Tryk *et al.*, 2000].

Photocatalysis is defined by Kirsch [1989] as ‘the acceleration of a photoreaction by the presence of a catalyst’. In simpler terms photocatalysis combines photochemistry and catalysis, and implies that light and a catalyst are required to accelerate a chemical transformation.

The process of photocatalysis involves the adsorption of photons by a molecule or the substrate to produce highly reactive electronically excited states [Linsebigler *et al.*, 1995]. The photon requires an energy of $h\nu$ that is either equal to or higher than its bandgap energy (E_{bg}) of the semiconductor in order to promote an electron (e^-) from the valence band (VB) to the conduction band (CB), creating an electronic vacancy or sometimes referred to as a positive hole (h^+) in the valence band. The E_{bg} is the energy difference that separates the VB and the CB [Robertson, 1996]. Excited state conduction band electrons and valence band holes can recombine and dissipate heat energy and become either trapped in metastable surface states or react with electron donors (D) and electron acceptors (A) absorbed on the semiconductor surface or within the surrounding electrical double layer of the charged particles. In the absence of suitable electron and hole scavengers the stored energy is dissipated by recombination. If a suitable scavenger or surface defect state is available to trap the electron or hole, recombination is prevented and subsequent redox reactions may occur. These events are illustrated in Figure 2.4.

Figure 2.4 Events that take place on a semiconductor in photocatalysis



Some of the reasons why photocatalysis is commonly used are because it offers the following distinctive advantages [Devahasdin *et al.*, 2003] when compared to competing technologies such as ultrafiltration, extraction, air stripping, carbon adsorption, incineration and oxidation via ozonation or via hydrogen peroxide [Serpone, 1995]:

1. Ability to oxidize low-concentration and low-flow rate waste streams at, but not limited to, ambient temperatures and pressures.
2. Ease of operation (instant on/off), modularity, and portability.
3. Complete mineralization for hydrocarbons.
4. By-products amenable to bio-remediation for oxygenates.
5. Potential utilization of solar energy with semiconductor particles (e.g. TiO_2) with a mechanism similar to that of photosynthesis in green plants.

2.3.2 Common photocatalytic applications

Under the illumination of ultraviolet light, photocatalysis shows diverse functions, such as the decomposition of air and water contaminants and deodorization, as well as self cleaning, antifogging, and antibacterial actions (Table 2.2). Practical applications of photocatalysts have rapidly expanded in recent years. Photocatalytic materials for outdoor purification are in urgent demand because energy and labour saving advantages have been realized when applied to building or road construction materials in large cities where local pollution is very serious [NAIST, 2001].

2.3.3 Application of photocatalyst in construction materials

Lackhoff *et al.* [2003] demonstrated that in concrete the addition of TiO₂ at 10 % by weight of cement improved the compressive strength of cubes after 28 days of curing, with P25 TiO₂ from Degussa Company performing the best in strength improvement, compressive strengths increased by 20 %.

Murata *et al.* [1999b] have also successfully utilized this advantage to design an air-cleaning block named Noxer [MMC, 2005]. The Noxer consists of a TiO₂ surface layer, which claims to remove NO_x from the atmosphere [Murata *et al.*, 2002]. When the surface of the block is irradiated by sunlight, active oxygen is created on the surface of the block due to a reaction of ultraviolet light in the sunlight (refer to section 2.3.6) and TiO₂ contained within the block. Active oxygen has high oxidation efficiency and oxidizes NO_x in the air into nitrates. The resultant nitric acid is then washed away by rain. Any nitric acid ions remaining on the surface or permeating the block are neutralized by the alkaline nature of the concrete. It is therefore suggested that the Noxer can be used repeatedly without driving energy and little maintenance.

Table 2.2 Selected applications for photocatalysis [Fujushima *et al.*, 2000, Fujushima *et al.*, 1999 and Murata *et al.*, 1999b]

Property	Category	Application	Example
Self-cleaning	Indoor and outdoor building materials	Exterior tiles, kitchen and bathroom components, interior furnishings, plastic surfaces, aluminum siding, building stone and curtains, paper window blinds.	Photocatalytic tiles by Janis Co. Ltd. Aluminum siding on the Sendai YF building of the YKK corporation in Sendai, Japan
	Indoor and outdoor lamps and related systems	Translucent paper for indoor lamp covers, coatings on fluorescent lamps and highway tunnel lamp cover glass. Tunnel wall, soundproofed wall, traffic signs and reflectors. Tent material, cloth for hospital garments and uniforms and spray coatings and paints.	Self cleaning tent material for the batting practice center opposite the main railway station in Osaka, Japan
Air cleaning	Indoor air cleaners	Room air cleaner, photocatalyst equipped air conditioners and interior air cleaner for factories.	Air cleaning plants by G.B.S. Co. Ltd
	Outdoor air purifiers	Concrete and cement based sprays for highways, roadways and footpaths, tunnel walls, soundproof walls and building walls.	The Noxer paving block by Mitsubishi Materials Corporation Shotcrete-type sound and pollutant absorbing material by Nippon Tokushu Toryo Co. Photoroad cement based spray for paved road by Fujita Corp.
Anti-fogging		Road mirrors, bathroom mirrors, refrigerated showcases, heat exchangers for air conditioners and high voltage transmission equipment, inside surfaces of windows, glass films, rear view mirrors and wind shields, spray on antifogging coatings and films, general purpose paints and coatings, optical lenses.	Antifogging coatings by Marutake Sangyo Co. Ltd.
Water purification	Drinking water	River water, ground water, lakes and water storage tanks.	Glassware by The Japanese Ceramics Institute
	Other	Fish feeding tanks, drainage water and industrial waste water.	
Autitumor activity	Cancer therapy	Endoscopic like instruments.	
Self sterilizing	Hospital	Tiles to cover the floor and walls for operating rooms, silicone rubber for medical catheters and hospital garments and uniforms.	
	Others	Public rest rooms, bathrooms and rat breeding rooms.	
Stain proof		Plastic film to coat over kitchen appliances, spray paint coating for cars.	

Laboratory tests carried out by Murata *et al.* [1999b] indicated that 80 % of NO_x could be removed using the Noxer. Field tests [MMC, 2005] also indicated that when the amount of traffic was 6000 cars per day, 15 % of the NO_x emission can be removed by the photocatalytic paving. However field tests for the Noxer carried out by the Chinese University of Hong Kong showed that for blocks with four months exposure their activities dropped by 36 % to 80 %, and for blocks with twelve months exposure their activities dropped by 22 % to 88 % [Yu, 2003]. It was also observed that the accumulation of contaminants reduced the surface area of blocks, which reduced the reactivity. Washing with water had little recovery effect. The findings suggest that the Noxer should be used in places with heavy automobile traffic but away from human intrusion to avoid contamination.

2.3.4 Titanium dioxide (TiO₂)

Photocatalysis employs semiconductors such as SrTiO₃, TiO₂, ZnO, ZnS, and CdS as a photocatalyst. Amongst which TiO₂ possesses the highest photocatalytic activity and is one of the most widely used semiconductors for photocatalysis. This is mainly due to its activity, photostability, non-toxicity and commercial availability and being relatively cheap [Fujishima *et al.*, 2000]. A photocatalyst or photocatalytic material that can efficiently generate active oxygen species is considered to be a good photocatalyst [NIAST, 2001]. TiO₂ has been shown to be an effective way of removing organic hazardous compounds and pollutant gases from both air and aqueous environments [Dalton *et al.*, 2002].

TiO₂, which is one of the most basic materials in our daily life, the commercial production of this white pigment has been known since the early 20th century. In recent years it has emerged as an excellent photocatalyst material for environmental purification. TiO₂ can clear the air because it is an efficient photocatalyst, with the aid of ultraviolet light. The results of the reaction are hydroxyl radicals, which attack both inorganic and organic compounds, and turn them into molecules that can be harmlessly washed away with the next rainfall when applied outdoors [Chan *et al.*, 2001]. Photocatalysts are not especially useful for breaking down large volumes of soilage, but they are capable of destroying it as it accumulates. TiO₂ photocatalysts thus hold great potential as quiet, unobtrusive self-cleaning materials [Wong and Tanner, 1997]. The photocatalytic technology requires no driving energy, minimal maintenance actions and can work throughout the year. One of the reasons TiO₂ is widely welcomed is due to its ability to be activated repeatedly, as TiO₂ is a catalyst it does not change after chemical reaction.

It has been shown that the photocatalytic effect of TiO₂ is dependent on crystal structure, particle size and surface area and that the effectiveness of the process is governed by the lifetime, or recombination probability, of the electron-hole pair [Dalton *et al.*, 2002]. TiO₂ is found in nature and can exist in three crystal modifications, rutile, anatase and brookite. However, only the rutile and anatase play a role in the application of TiO₂ photocatalysis [Diebold, 2003]. The rutile form is generally less photoactive compared to the anatase form, as it has a lower

capacity to adsorb O₂ and therefore the electron-hole recombination rate is higher [Fox and Dulay, 1993].

The diameter of its particles usually lies between 25 nm and 35 nm. Hence the separation of TiO₂ nano-particles from its aqueous suspensions represents a serious problem for practical engineering. Therefore a key technique for simple applications seems to be the preparation of immobilized TiO₂ coatings on different substrates (glass sheets, tiles etc.) without loss of photocatalytic activity.

The effects of the nature and of the source of various TiO₂ specimens have been explored extensively. Hombikat UV-100 TiO₂ (Sachteleben Chemie GmbH, Duisburg, Germany) consists of pure anatase modification and its particles have a BET specific surface area of about 186 m²g⁻¹ [Oppenlander, 2003], compared to the typical range of 10-300 m²g⁻¹. However the majority of investigations have been performed using P-25 TiO₂ from Degussa company due to its high reactivity, it contains a high TiO₂ content of 99.50% and because it is commonly used and recognized by people in the industry and research, hence is useful for comparison with works of others. This material consists of about 80 % anatase and 20 % rutile and has a BET specific surface area of ca. 55 m²g⁻¹ [Oppenlander, 2003]. For certain photocatalytic reactions such mixtures work best [Diebold, 2003]. P-25 TiO₂ seems to be superior over synthetic sol-gel TiO₂ with respect to the photocatalytic activity for degradation of organic substrates [Oppenlander, 2003] (Refer to section 3.1.2 for properties of P-25).

2.3.5 *Methods of applying photocatalyst*

There are many ways that TiO₂ photocatalyst can be applied such as flame synthesis [Pratsinis, 1996], magnetron sputtering [Baroch *et al.*, 2004], chemical vapour deposition [El-Sheikh *et al.*, 2004], sol-gel [Jung and Park, 2004], spraying [Nonoyama and Kogo, 2000] and mixing [Kamiya *et al.*, 1998].

Applying a photocatalyst by mixing is much simpler, time consuming and cheap compared to the other methods. Kamiya *et al.* [1998] demonstrated that TiO₂ could be mixed with cement to produce a cement based hydraulic composition for NO_x purifying.

In addition, Murata *et al.* [1999b] designed paving blocks by mixing aggregates, TiO₂, cement and water. Their study showed that the block removed NO under a range of different environment conditions such as light intensity and humidity.

Lackhoff *et al.* [2003], produced photocatalyst modified cements for building and environmental technologies, by mixing cement and TiO₂. Their study showed that it was feasible to produce modified cement with photocatalytic properties for the removal of atrazine.

Nonoyama and Koga [2004], also prepared a mixture of TiO₂, cement, a filler and water. Although the materials were also prepared by mixing, the mixture was

sprayed onto the surface of roads to purify exhaust gases emitted from vehicles, by photocatalytic reaction of the photocatalyst.

2.3.6 Removal of NO using TiO₂ photocatalysis

TiO₂ is considered to be a promising material for treatment of air pollutants through its highly strong oxidative ability. It showed the highest photocatalytic activity for oxidation of SO₂ and NO₂ to sulphuric acid (H₂SO₄) and nitric acid (HNO₃). This suggests that TiO₂ can be used as a photocatalyst for removing ambient SO₂ and NO_x [Okura and Kaneko, 2002]. For example TiO₂ has already been commercially exploited both in UK and Japan for concrete paving materials in inner cities due to its ability to remove NO_x [Dalton *et al.*, 2002]. Japan was the first country to apply TiO₂ photocatalysis and is also the most active country in this field.

Takashi and Takeuchi [1994] used a flow type photochemical reaction system to demonstrate that rapid photocatalytic oxidation of NO to NO₂ and HNO₃ using P-25 TiO₂ powders from Degussa Company. The reactor consisted of a pyrex glass cylinder which was coated with the catalyst powder on the inner surface, and then placed into an outer cylinder. Photoillumination was provided by 12 black lights on the exterior whilst the testing gas was passed through the reactor.

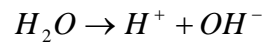
Experiments of photodegradation of NO by TiO₂ showed that NO₂ is the only intermediate under the presence of oxygen, and NO₂ can further be photooxidised to

HNO₃, this mechanism can be expressed by the following equations [Dalton *et al.*, 2002, Devahasadin *et al.*, 2003, Okura and Kaneko, 2002 and Komazaki *et al.*, 1999]:

1. When TiO₂ is illuminated by light with wavelengths below 400 nm it generates excitons of positive holes (h^+) and photoelectrons (e^-), which catalyze both oxidation and reduction reactions.



2. Water adsorbed by the TiO₂ leads to the formation of highly hydroxylated surface and also gives hydrogen ions (H^+) and hydroxide ions (OH^-) by its dissociation.

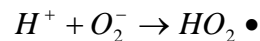


3. The h^+ reacts with OH^- to generate $OH\bullet$ on the surface of TiO₂.

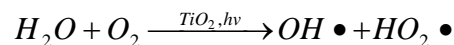


4. Meanwhile e^- is free to participate in the adsorption of oxygen from air and produces O_2^- on the TiO₂ surface.

5. O_2^- is followed by the reaction with H^+ and forms $HO_2\bullet$.

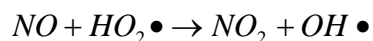


6. The reaction overall can therefore be expressed as the below.



7. NO diffuses to the surface of TiO₂ and rapidly reacts with $HO_2\bullet$ to produce

NO₂ as well as the photochemical reactions in the atmosphere.



8. NO₂ further reacts with OH• to form HNO₃.



However Diebold [2003] and Zhang *et al.* [2001] reported from their studies that the products from NO photodegradation were N₂, O₂ and N₂O under the presence of helium instead of oxygen. Oxygen acts as the primary electron acceptor during the photodegradation of NO when under the presence of oxygen [Hoffmann *et al.*, 1995]. As a result oxygen was primary reduced to superoxide and NO was oxidized to NO₂ and further oxidized to HNO₃. But NO photodegradation under the presence of helium oxidized to O₂ and reduced to N₂O and N₂.

3. Methodology

3.1 Materials

3.1.1 Cement

The cementitious material used in this study was an Ordinary Portland Cement (OPC), complying with BS 12 [BS, 1996] and ASTM Type I [ASTM, 2004]. This type of OPC is commercially available in Hong Kong and is often used as the setting agent for general concrete works such as for floors, reinforced concrete structures, pavements etc. The properties of the OPC are shown in Table 3.1.

3.1.2 Titanium dioxide (TiO₂)

TiO₂ is often used as a catalyst in photocatalysis for environmental purification. The use of TiO₂ has been shown to be an effective way of removing organic poisonous compounds and pollutant gases from both air and aqueous environments [Dalton, 2002]. Three sources of TiO₂ were used in this study. P-25 sourced from Degussa Company. P-25 was used due to its high purity, accurate specifications, and because it is commonly used and recognized by people in the industry and research, hence would be useful for comparison with works of others. The two other types of TiO₂ were sourced from Ke Xiang a chemical products company in Shanghai of China

due to their low prices compared to P25. The two types of TiO_2 included one in the form of anatase crystal structure and the other in the form of rutile crystal structure. The two types of TiO_2 are referenced as anatase and rutile respectively in this study. The properties of TiO_2 are shown in Figures 3.1 and 3.2, and Table 3.2.

Figure 3.1 Particle size distribution of TiO_2 powders

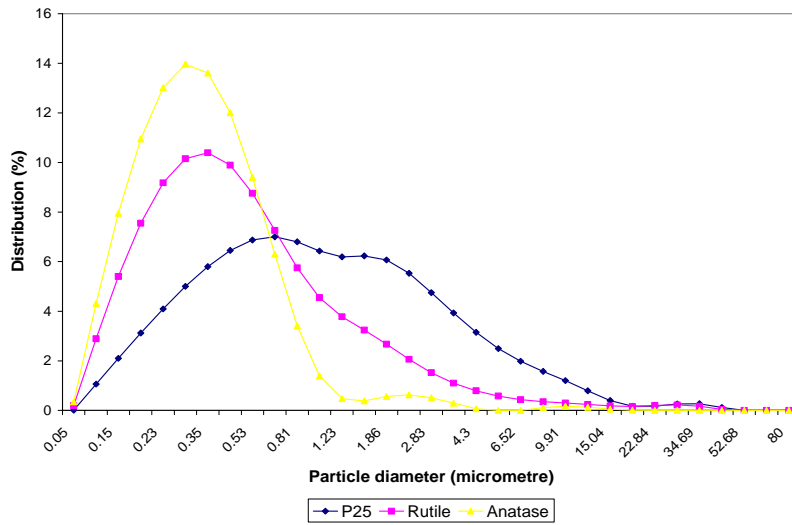
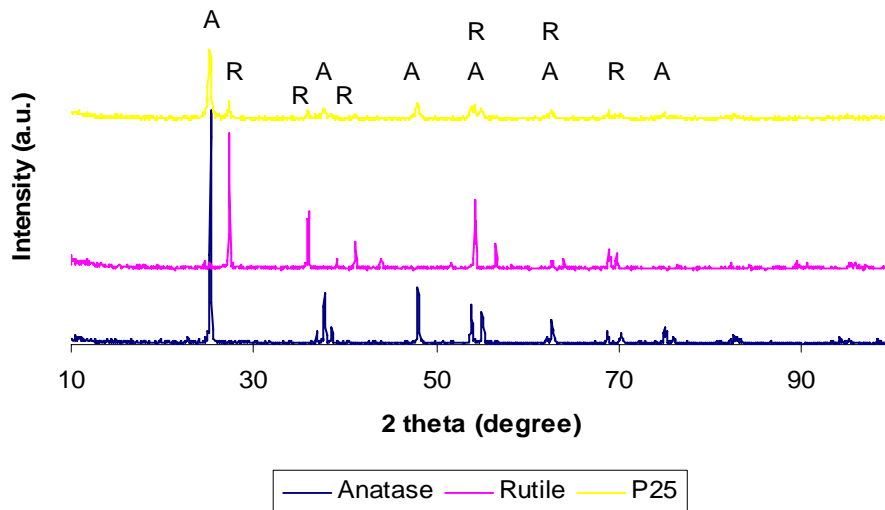


Figure 3.2 XRD spectrum of TiO_2 powders (A: Anatase, R: Rutile)



3.1.3 Furnace bottom ash (FBA)

Furnace bottom ash (FBA) is a by-product of coal-fired electricity generation. FBA is the coarser material that falls to the bottom of the furnace during the burning of coal. Chemically, it is very similar to pulverized fly ash but due to its coarse grain size, it is not commonly used in cement and concrete applications [Dawson, 1991 and Kayabali and Bulus, 2000]. In Hong Kong the produced FBA is currently dumped at an ash lagoon as waste. FBA used in this study was sieved in the laboratory and only the portion that passed through a 2.36 mm sieve was used for making the surface layer. The specific density was 1877 Kgcm^{-3} . The properties of the FBA are similar to PFA.

3.1.4 Pulverised fly ash (PFA)

Pulverised fly ash (PFA) is also a by-product of coal-fired electricity generation, but it is the finer material that is transported by the flue gases to the particle removal system, where it is collected. Unlike FBA, PFA is commercially available. Low calcium pulverized fly ash (PFA) equivalent to ASTM Class F [ASTM, 2003a] from a local source was used in this study. The properties of the PFA are shown in Table 3.1.

3.1.5 Metakaolin (MK)

Metakaolin (MK) is a thermally activated alumino-silicate produced from kaolinite clay through a calcining process. Similar to silica fume it reacts aggressively with calcium hydroxide and hence is used as a supplementary cementitious material with pozzolanic properties. The addition of MK in concrete is visually appealing as the colour is lightened due to MK's white nature. The same source of MK was used in a previous study [Poon *et al.*, 2001a] and the properties have been given (Table 3.1).

Table 3.1 Properties of OPC, PFA and MK

Properties	OPC	PFA	MK
SiO ₂ (%)	19.61	56.79	53.20
Fe ₂ O ₃ (%)	3.32	5.31	0.38
Al ₂ O ₃ (%)	7.33	28.21	43.90
CaO (%)	63.15	<3	0.02
MgO (%)	2.54	5.21	0.05
SO ₃ (%)	2.13	0.68	-
Na ₂ O (%)	-	-	0.17
K ₂ O (%)	-	-	0.10
TiO ₂ (%)	-	-	1.68
Loss on ignition (%)	2.97	3.90	0.50
Density (Kgcm ⁻²)	3160	2310	2620
Specific surface area (cm ² g ⁻¹)	3520	3960	12680

Table 3.2 Properties of TiO₂

Properties	P25	TA	TR
Moisture (%)	<1.5	<0.04	<0.46
Water solubility (%)	-	0.05	0.03
Ignition loss (%)	<2.0	<0.01	<0.17
pH	3.0~4.0	7.5	6.7
Oil adsorption (g/g)	-	22/100	23/100
Color eliminating capacity (per min)	-	100	100
Sieve residue, Mocker>45 (%)	<0.05	0.05	0.05
TiO ₂ (%)	>99.5	98.5	91

3.1.6 Recycled aggregates (RA)

The RA used in this study was crushed and sorted C&D wastes sourced from Tuen Mun Area 38, which is a temporary recycling facility for C&D waste in Hong Kong. In the plant the C&D waste underwent a process of mechanized crushing and sieving to produce both fine and coarse aggregates according to the particle size requirements of BS 812 [BS, 1985] and to remove excess impurities which would affect the performance of the aggregates. Only the fine aggregate proportion was used for making the surface layer of the blocks. The maximum nominal size of the recycled fine aggregate used was 2.36 mm with a specific density of 2093 Kgcm⁻³. The recycled coarse aggregate was also incorporated into the mix design for the base layer of the blocks. The properties of the RA are shown in Table 3.3.

3.1.7 Recycled glass (RG)

The RG used in this study was mainly post-consumer beverage bottles sourced locally. The glass bottles were washed, sorted by color and crushed by mechanical equipment. The RG was sieved in the laboratory to achieve a maximum nominal size of 2.36 mm. The properties of the RG are shown in Table 3.3.

3.1.8 Sand

The sand used was fine natural river sand commercially available in Hong Kong. The specific density of the sand used was 2651 Kgcm⁻³. The properties of sand are shown in Table 3.3.

Table 3.3 Properties of RA, RG and sand

Properties	RA (fine)	RA (coarse)	RG	Sand
Saturated surface dry density (Kgcm ⁻³)	2308	2581	2590	2643
Specific density (Kgcm ⁻³)	2093	2523	2531	2651
Water absorption (%)	10.28	2.29	0	0.87

3.2 Mix proportions

3.2.1 Mix proportions prepared with RA, FBA and sand

Porosity was believed to be an essential property for the high activity of pollutant removal. A paving block with high porosity effectively increases its adsorption area available to pollutants. The increased number of active sites due to higher porosity allows pollutants to be removed more efficiently. Therefore it was important to investigate the optimum level of porosity allowing efficient pollutant removal but at the same time not affecting the physical properties of the paving block allowing it to perform its designed role.

When considering the factors affecting a paving block's porosity the choice of material used was important. The density of a material could be considered as one of the reasons contributing to the paving block's porosity hence materials possessing lower densities were considered more favorable. This study focuses on utilizing recycled materials, so the materials selected for trial included the recycled materials FBA, RA and RG, and sand as the natural material for comparison purposes. Amongst the materials selected FBA possesses the lowest specific density of only 1877 Kgcm^{-3} . Therefore, on the basis of the previous assumption paving blocks comprising FBA should be more efficient at removing pollutants compared to the other materials selected.

In addition another possible factor affecting the paving block's porosity and as a result the photodegradation of NO was the cement to aggregate ratio of the paving block. Changing the cement to aggregate ratio affectively alters the porosity content of the blocks. Cement is a fine material which can easily fill up pore spaces, and hence reduce the effective areas for pollutant adsorption. When the cement content is decreased the surface area available is effectively increased, hence the removal ability of pollutants is more efficient.

The curing age of the paving blocks as well as the particle size of the materials used in the paving blocks were also factors considered to affect the porosity of paving blocks, as with increasing curing age, changes in cement hydration were believed to affect the surface area available to pollutants and more obvious the choice in particle size of the paving block materials was also believed to affect the surface area available. Hence the mix proportions shown in Tables 3.4-3.7 were designed to analyze the factors of consideration.

Table 3.4 Mix proportions of cubes prepared with RA and FBA

Mix notation	Proportion (Kg)			
	Cement	RA (fine)	FBA	Water
FBA-0	1	2	0	0.33
FBA-25	1	1.5	0.5	0.35
FBA-50	1	1	1	0.36
FBA-75	1	0.5	1.5	0.38
FBA-100	1	0	2	0.39

Table 3.5 Mix proportions of surface layers prepared with RA, FBA and varying TiO₂

Mix notation	Proportion (Kg)				
	Cement	RA (fine)	FBA	TiO ₂	Water
FBA-75-0	1	0.5	1.5	0	0.38
FBA-75-2	1	0.5	1.5	0.02	0.38
FBA-75-4	1	0.5	1.5	0.04	0.40
FBA-75-6	1	0.5	1.5	0.06	0.40
FBA-75-8	1	0.5	1.5	0.08	0.42
FBA-75-10	1	0.5	1.5	0.10	0.42

Table 3.6 Mix proportions of surface layers prepared with RA, FBA and sand

Mix	Proportion (Kg)					
	Cement	RA	Sand	FBA	TiO2	Water
R1:2	1	2	-	-	0.06	0.28
R1:2.5	1	2.5	-	-	0.07	0.30
R1:3	1	3	-	-	0.08	0.32
R*1:2	1	2	-	-	0.06	0.28
R*1:2.5	1	2.5	-	-	0.07	0.30
R*1:3	1	3	-	-	0.08	0.32
S1:2	1	-	2	-	0.06	0.24
S1:2.5	1	-	2.5	-	0.07	0.26
S1:3	1	-	3	-	0.08	0.28
S*1:2	1	-	2	-	0.06	0.24
S*1:2.5	1	-	2.5	-	0.07	0.26
S*1:3	1	-	3	-	0.08	0.28
RF1:2	1	1.5	-	0.50	0.06	0.32
RF1:2.5	1	1.88	-	0.63	0.07	0.34
RF1:3	1	2.25	-	0.75	0.08	0.36
RF*1:2	1	1.5	-	0.50	0.06	0.32
RF*1:2.5	1	1.88	-	0.63	0.07	0.34
RF*1:3	1	2.25	-	0.75	0.08	0.36
SF1:2	1	-	1.5	0.50	0.06	0.28
SF1:2.5	1	-	1.88	0.63	0.07	0.30
SF1:3	1	-	2.25	0.75	0.08	0.32
SF*1:2	1	-	1.5	0.50	0.06	0.28
SF*1:2.5	1	-	1.88	0.63	0.07	0.30
SF*1:3	1	-	2.25	0.75	0.08	0.32

(All mix proportions were prepared with aggregate sizes below 2.36 mm only, except those identified by ‘*’ were prepared with aggregate sizes between 300 µm to 2.36 mm)

Table 3.7 Mix proportions of cubes prepared with RA, FBA and sand

Mix	Proportion (Kg)					
	Cement	RA (fine)	Sand	FBA	TiO ₂	Water
R1:3	1	3	-	-	0.08	0.32
R*1:3	1	3	-	-	0.08	0.32
S1:3	1	-	3	-	0.08	0.28
S*1:3	1	-	3	-	0.08	0.28
RF1:3	1	2.25	-	0.75	0.08	0.36
RF*1:3	1	2.25	-	0.75	0.08	0.36
SF1:3	1	-	2.25	0.75	0.08	0.32
SF*1:3	1	-	2.25	0.75	0.08	0.32

3.2.2 Mix proportions prepared with RG

The light transmitting characteristic of glass was believed to benefit NO photodegradation when used in the mix design of the paving blocks. Hence mix proportions prepared with recycled glass were designed (Tables 3.8-3.10).

In this study four sources of recycled glass were used. A transparent recycled glass sourced from a local sauce manufacturer (used in all mixes prepared with recycled glass except Table 3.9), another transparent glass sourced from crushed milk bottles (denoted by 'T'), and also a green and a brown colored glass both mainly from crushed beverage bottles (denoted by 'G' and 'B' respectively).

The optimum mix prepared with recycled glass was also analysed for alkali silica reaction (ASR), as ASR is often a concern in cement mixtures containing glass. So mix designs with the addition of fly ash or metakaolin were prepared.

Table 3.8 The mix proportions of cubes and surface layers prepared with RG

Mix	Proportion (Kg)				
	Cement	RG	Sand	TiO ₂	Water
GS100	1	3	-	0.08	0.28
GS75	1	2.25	0.75	0.08	0.28
GS50	1	1.5	1.5	0.08	0.28
GS25	1	0.75	2.25	0.08	0.28
GS0	1	-	3	0.08	0.28

Table 3.9 Mix proportions of cubes and surface layers prepared with different RG

Mix	Proportion (Kg)				
	Cement	RG	Sand	TiO ₂	Water
GS50(T)	1	1.5	1.5	0.08	0.28
GS50(G)	1	1.5	1.5	0.08	0.28
GS50(B)	1	1.5	1.5	0.08	0.28

Table 3.10 Mix proportions of mortar bars and surface layers prepared with MK and PFA

Mix	Proportion (Kg)					
	Cement	RG	Sand	TiO ₂	Additive	Water
MK2.5	1	1.5	1.5	0.08	0.075	0.28
MK5	1	1.5	1.5	0.08	0.15	0.30
MK10	1	1.5	1.5	0.0	0.30	0.32
PFA2.5	1	1.5	1.5	0.08	0.075	0.28
PFA5	1	1.5	1.5	0.08	0.15	0.30
PFA10	1	1.5	1.5	0.08	0.30	0.32

3.2.3 Mix proportions prepared with TiO₂

Further mix proportions were prepared to analyze the ability of TiO₂. A mix design was selected from section 3.2.2 from the results achieved and used to prepare specimens with the TiO₂ content ranging from 0 % to 10 % at 2 % intervals (Table 3.11).

In order to improve the NO removal ability, the recycled glass was coated with the assistance of The Chinese University to analyze the effect when used in the mix design replacing the ordinary recycled glass. The mix proportions of specimens prepared with coated recycled glass cullets were designed and compared with previous results (Table 3.12).

Before coating the glass cullets were prepared by sieving, washing and drying. Using this coating methodology the glass cullets were sieved to sizes of 1-2 mm because only at these sizes could the cullets be properly coated. The sieved cullets were further put through a washing process. Acid was passed through the cullets followed by water twice, distilled water was further passed through the cullets and finally ethanol was also passed through the cullets. After the cullets were washed they were oven dried at 100 °C which concluded the preparation. To coat the cullets a funnel and filter paper were used. The cullets were placed in the filter paper and a previously prepared solution was passed through the cullets twice. The solution was prepared with 10 % Titanium (IV) Isopropoxide ($\text{Ti}[\text{OCH}(\text{CH}_3)_2]_4$) with a density of 0.963 and a molecular weight of 284.26. The resultant coating was approximately 220 nm thick. To ensure that the coating stays on the glass cullets they were oven dried at 100 °C for 10-15 minutes and then at 500 °C for an hour.

Specimens were designed and prepared with different sources of TiO_2 for comparison, the TiO_2 contents of these different sources were also varied similar to mixes in Table 3.8 (Tables 3.13 and 3.14).

Table 3.11 Mix proportions of cubes and surface layers with varying TiO₂ content

Mix	Proportion (Kg)				
	Cement	Glass	Sand	TiO ₂	Water
0%	1	1.5	1.5	0	0.26
2%	1	1.5	1.5	0.08	0.28
4%	1	1.5	1.5	0.16	0.36
6%	1	1.5	1.5	0.24	0.40
8%	1	1.5	1.5	0.32	0.48
10%	1	1.5	1.5	0.40	0.64

Table 3.12 Mix proportions of surface layers prepared with coated glass

Mix	Proportion (Kg)					
	Cement	RG	Coated glass	Sand	TiO ₂	Water
Control	1	1.5	-	1.5	0.08	0.28
Coated	1	-	1.5	1.5	-	0.28
P25	1	1.5	-	1.5	0.08	0.28
Coated+P25	1	-	1.5	1.5	0.08	0.28

Table 3.13 Mix proportions of surface layers prepared with different sources of TiO₂

Mix	Proportion (Kg)						
	Cement	Glass	Sand	P-25 TiO ₂	Anatase TiO ₂	Rutile TiO ₂	Water
P-25	1	1.5	1.5	0.08	-	-	0.26
Anatase	1	1.5	1.5	-	0.08	-	0.26
Rutile	1	1.5	1.5	-	-	0.08	0.26

Table 3.14 Mix proportions of surface layers prepared with varying anatase and rutile TiO₂ contents

Mix	Proportion (Kg)				
	Cement	Glass	Sand	TiO ₂ (Anatase/Rutile)	Water
0%	1	1.50	1.50	0	0.26
2%	1	1.50	1.50	0.08	0.28
4%	1	1.50	1.50	0.16	0.36
6%	1	1.50	1.50	0.24	0.40
8%	1	1.50	1.50	0.32	0.48
10%	1	1.50	1.50	0.40	0.64

3.3 Sample preparation

3.3.1 Fabrication of cubes

The compressive strength of the mix designs were derived by testing the strength of cubes which were fabricated in steel moulds with internal dimensions of 70x70x70 mm (Figure 3.3). The wet mixed materials weighed between 600 to 780 g for each cube depending on the different materials. The steel moulds were over filled by hand hammer compaction in three layers, and then further compressed using a compression machine at a rate of 600 KN per minute twice, firstly to 500 KN and secondly to 600KN. After one day, the cubes were removed from their moulds and cured in a chamber for a further 27 days with a controlled humidity of 75 % and temperature of 25 °C. At 28 days the cubes were tested for compressive strength.

Figure 3.3 Cube moulds



3.3.2 *Fabrication of surface layers*

Surface layers for the different mix designs were prepared to test for NO photodegradation. The surface layers were fabricated in steel moulds with internal dimensions of 200x100x5 mm (Figure 3.4). The wet mixed materials weighed between 220 to 280 g for each surface layer depending on the different materials. The steel moulds were over filled by hand compaction, and then further compressed using a compression machine at a rate of 600 KN per minute twice, first to 500 KN and secondly to 600KN. After one day, the surface layers were removed from their moulds and cured in a chamber with a controlled humidity of 75 % and temperature of 25 °C until testing. The surface layers were tested for NO photodegradation at 7, 28, 56 and 90 days.

Figure 3.4 Surface layer moulds



3.3.3 Fabrication of paving blocks

Paving blocks for selected mix designs were prepared and tested for their physical properties as well as for NO_x photodegradation. Steel moulds with internal dimensions of 200x100x60 mm (Figure 3.5) were used for fabrication. The paving blocks were prepared in two layers, a base layer and a surface layer. The wet mixed materials for the base layer weighed 2800 g and was filled into the steel moulds in three layers by hand hammer compaction, and then further compressed with a self designed mould on top to indent space for the surface layer (Figure 3.6). The compression was carried out using a compression machine at a rate of 600 KN per minute to 600 KN once. The top mould was taken off the block mould and the wet mixed materials (260g) for the surface layer were filled in and compacted by hand. The blocks were then further compressed using the same compression machine at a rate of 600 KN per minute twice, first to 500 KN and secondly to 600 KN. After one day, the blocks were removed from their moulds and cured in a chamber with a controlled humidity of 75 % and temperature of 25 °C until testing. The tests performed on the blocks are described in section 3.4 of Chapter 3.

Figure 3.5 Paving block moulds



Figure 3.6 Indention mould for paving blocks



3.3.4 Fabrication of mortar bars

The alkaline silica reaction of the mixes prepared with the incorporation of recycled crushed glass were tested by measuring the expansion of the prepared mortar bars after being soaked in a sodium hydroxide solution for different times. The preparation method of the mortar bars followed a similar method as in ASTM C1260-01 [2001] but with alterations. The requirements for the steel moulds were

the same with internal dimensions of 285x25x25 mm (Figure 3.7). But the material size, cement ratio and water to cement ratio were altered according to the mix designs. Due to the alterations the wet mixture had to be compacted using hand hammer in three layers and further compacted using a compression machine at a rate of 600 KN per minute twice, first to 500 KN and secondly to 600 KN. The mortar bars were demoulded the following day and soaked in a water bath at 80 °C for 24 hours before soaking in the sodium hydroxide solution also at 80 °C until measurement.

Figure 3.7 Mortar bar moulds



3.4 Determination of physical properties

3.4.1 Compressive strength

The compressive strength of the specimens was determined using a Denison compression machine with a maximum capacity of 3000 KN, according to BS 6717 [1993]. Before loading the specimens were packed with plywood top and bottom. The compression load was then applied to the face with a nominal area of 200x100 mm at a rate of 400 KN per minute until the specimens failed (Figure 3.8). The compression strength was determined by dividing the maximum load by the load area of the specimen.

Figure 3.8 Specimen being tested for compressive strength



3.4.2 Density

The density of the specimens was determined using the water displacement method, which is calculated by dividing the mass of specimens in air by the difference in mass of the specimens in air and water.

3.4.3 Water absorption

Water absorption of the specimens was determined according to AS/NZS 4456.14 [2003]. The percentage of cold water absorption is determined by dividing the difference of the weights of specimens after being soaked in cold water and after oven dried by the weight of specimens after oven dried. The percentage of hot water absorption is determined similarly but using the weight of specimens after boiling instead of the weight of specimens after being soaked in cold water in the calculation.

3.4.4 Skid resistance

The surface frictional properties were determined using a British pendulum skid resistance tester (Figure 3.9) according to ASTM E303 [2003b]. The skid resistance of the specimen surface is expressed as the measured British Pendulum Number (BPN).

Figure 3.9 British pendulum skid resistance tester



3.4.5 Abrasion

The abrasive resistance of specimens was determined by measuring the groove on the block surfaces after abrading with an abrasive material according to BS 6717 [2001]. The apparatus set up used to perform the abrading is shown in Figure 3.10.

Figure 3.10 Abrasion resistance apparatus



3.4.6 Porosity

The method requires the specimens to be crushed into approximately 10mm diameter sizes and then oven dried at 105 °C for 24 hours. 100 g of the prepared specimens were soaked in acetone in a sealed container for a day. The specimens were then removed from the acetone and the specimen surfaces were dried. The weights of the specimens were then weighed and the difference between the original weights indicated the amount of acetone that can be absorbed by the specimen per 100 g, which is also an approximate indication of the porosity of the specimens.

3.4.7 Alkaline silica reaction (ASR)

The potential alkaline silica reaction (ASR) expansion of the mixes prepared with the addition of recycled glass was determined according to ASTM C1260 [2001]. The mortar bars were soaked in a water bath at 80 °C for 24 hours before soaking in the sodium hydroxide solution also at 80 °C until measurement. The mortar bars were measured for expansion at 1, 3, 7, 10, 14 and 28 days.

3.4.8 X-ray diffraction (XRD)

The Bruker D8 Advance Powder Diffractometer (Figure 3.11) was used to analyze the different TiO₂ samples used in this study. The machine allowed the samples to be analysed in their existing powder form, hence no preparation was required.

Figure 3.11 Bruker D8 Advance Powder Diffractometer



3.4.9 Particle size distribution of TiO₂

The Mastersizer from Malvern Instruments Company was used to measure the particle size distribution of the different TiO₂ samples. A gram of the sample and 30 ml of distilled water was weighed into a beaker and shook for 20 minutes in a supersonic shaker. 3 ml of the solution was then placed into the machine for testing.

3.5 Photodegradation of NO

3.5.1 Apparatus

The testing equipment used is a self-designed flow reactor. The reactor provides a physical boundary to enable a photocatalytic material, in our case a photocatalytic block, to be examined for its pollutant removal capability. The reactor consists of a sampling inlet and outlet, and ultraviolet lamps to provide photoirradiation to activate the photocatalyst. The design enables the reactor to be used as a continuous flow reactor or a batch flow reactor. The reactor needed to be constructed with materials of low adsorption ability and resistance to ultraviolet irradiation, hence stainless steel and glass were chosen.

3.5.1.1 Original design

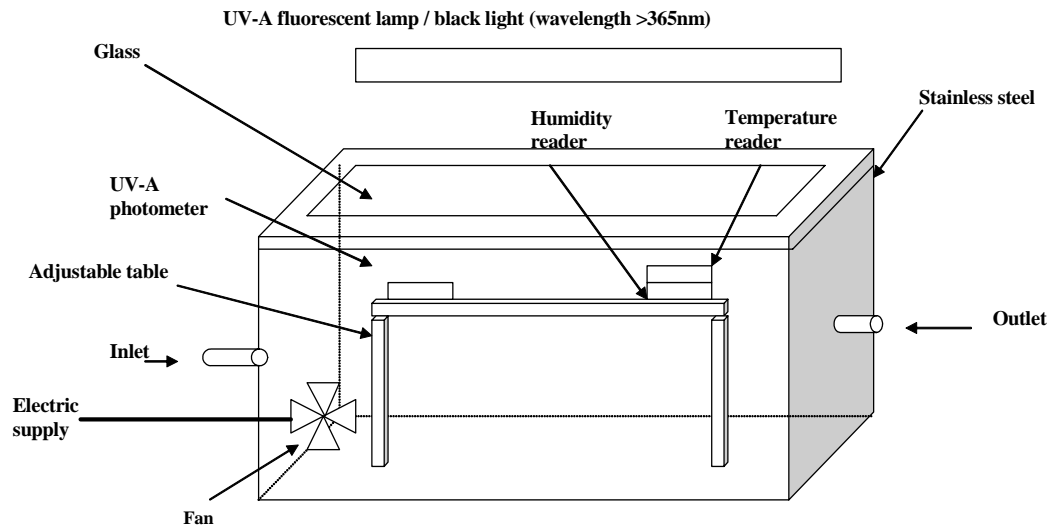
The size and materials used for the original reactor was adapted from an existing design [NAIST, 2001], but with alterations. The reactor was constructed using stainless steel of dimensions 700 mm in length, 400 mm in width and 400 mm in height (Figure 3.12). The size of the reactor had to be large enough to hold the samples as well as the reactor components. Rubber was used as sealant for the reactor. The lid of the reactor was designed using transparent glass rimmed with stainless steel. Illumination was provided by four 10 W UV-A fluorescent lamps (black lights), which emit primary UV light wavelengths at 365 nm similar to Yu

[2003]. The intensity was measured using a UV meter (Spectroline DRC-100X) to be 15 Wm^{-2} at the centre of the reactor. The light source was positioned outside the reactor and the distance from the reactor was adjusted till the required intensity was achieved. A temperature sensor, humidity sensor, fan (for circulation), and adjustable rack to support the specimens were placed inside the reactor. Figure 3.13 shows a schematic diagram of the reactor.

Figure 3.12 Original reactor design



Figure 3.13 Schematic diagram of the reactor



3.5.1.2 Revised design

The main reason for the revised design was because it was noticed that testing with the original design was too time consuming. It took double the amount of time for gas to fill up the reactor and also gas circulation was more difficult in a larger reactor. Therefore the design was revised with reduced dimensions (700 mm in length, 400 mm in width and 130 mm in height (Figure 3.14). The design of the reactor was similar to the original design except that two UV lamps were used to provide illumination for photocatalytic reaction to produce an intensity of 10 Wm^{-2} at the centre of the reactor, which was also where the test samples were placed. Similar to the original design a temperature sensor, humidity sensor, fan, and adjustable rack to support the specimens were placed inside the reactor.

Figure 3.14 Revised reactor design



3.5.2 Preliminary tests

The following tests were performed on the reactors to ensure that they would be suitable for its designed purpose.

1. Air leakage test – The reactor was tested for air leakage by introducing a small pressure at one outlet and taking the reading of the pressure at another outlet to ensure that the pressure reading balanced. Water was also squirted around the exterior of the reactor whilst pressure was introduced to look for leakage areas, which should create bubbles if any.
2. Time for NO in reactor to reduce to zero – Zero gas was generated and introduced into the reactor and the time required for NO to reduce to zero was recorded.

3. Time for reactor to reach NO gas status – The reactor was purged with zero air before introducing NO gas. The time taken for NO gas to completely fill the reactor was recorded.
4. Blank test – Testing was performed with no sample in the reactor, the results showed that in batch testing there was a predicted slight drop in NO level and believed not to effect other results as long as this was accounted for in the calibration. The drop is believed to be due to absorption from the reactor itself and the components within, which is common in a batch process. But similar to other studies tested under continuous mode, no NO photolysis was observed [Devahasdin *et al.*, 2003].
5. Calibration of Chemiluminescence NO analyzer – Different NO concentration levels were passed through the reactor and measured at the sampling outlet using a Chemiluminescence NO analyzer. The difference between the initial concentration and measured concentration was recorded and accounted for in the calibration.

3.5.3 Testing procedure

3.5.3.1 Original procedure

NO was used as the testing pollutant in this study as previous studies have shown that TiO₂ can reduce the levels significantly. In addition NO_x is constituted of over 80% NO which can be oxidized to NO₂.

The reactor was connected to a supply of standard gas (NO) and a zero air generator (Thermo Environmental Inc. Model 111, Figure 3.15). The standard gas was obtained from a compressed gas cylinder with nitrogen as the balanced gas (NIST certified). The gas streams were then adjusted by the flow controllers to achieve an initial NO concentration of 1000 ppb and a flowrate of 6 Lmin⁻¹. The desired humidity of the flow was controlled by passing the zero air stream through a water bath, the amount of water in the bath controlled the humidity level achieved. After the inlet and the outlet NO concentrations had reached equilibrium (1 hour), the UV lamps were turned on to begin the removal process (2 hours). Figure 3.16 shows a schematic diagram of the experimental set-up. The tests were carried out in two modes, (i) continuously and (ii) batch-wise. In the continuous mode, the concentration of NO was continuously measured by a Chemiluminescence NO analyser (Thermo Environmental Instruments Inc. Model 42c, Figure 3.17), which monitored NO and NO₂ concentrations. In the batch mode the inlets and outlets of the reactor were closed before the lamps were turned on, and the concentration of NO was measured using the same method after a fixed removal (2 hours) duration.

Figure 3.15 Zero air supply (Thermo Environmental Instrument Inc. Model 111)



Figure 3.16 Schematic diagram of the experimental set-up for the original procedure

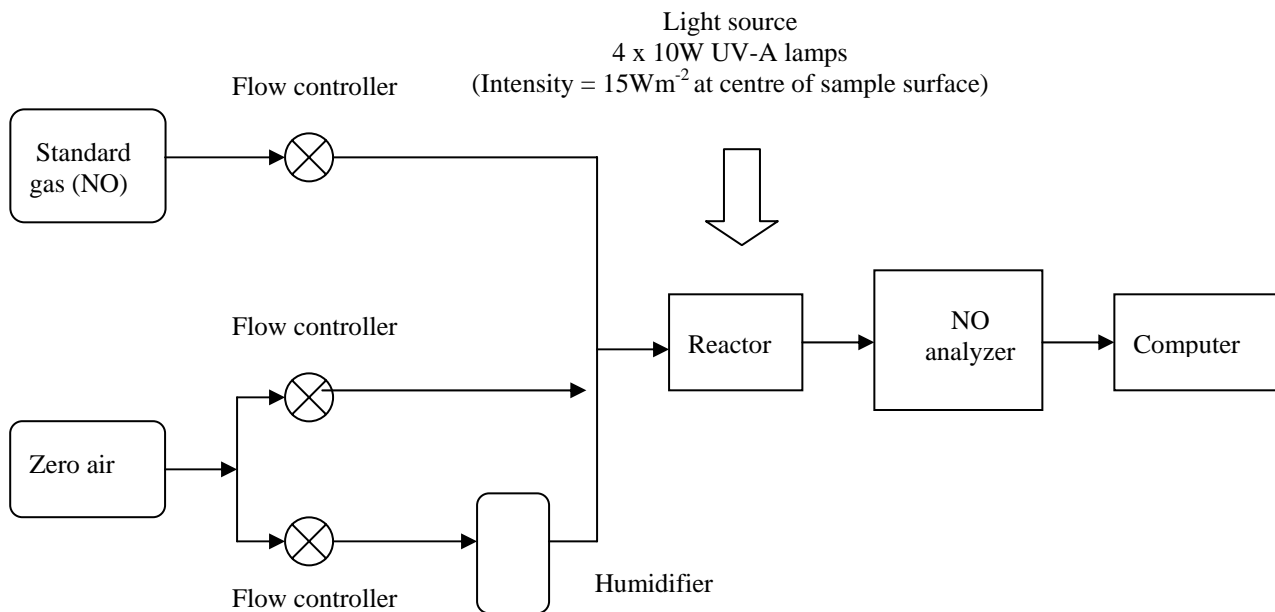


Figure 3.17 Chemiluminescence NO analyzer (Thermo Environmental Instrument Inc. Model 42c)

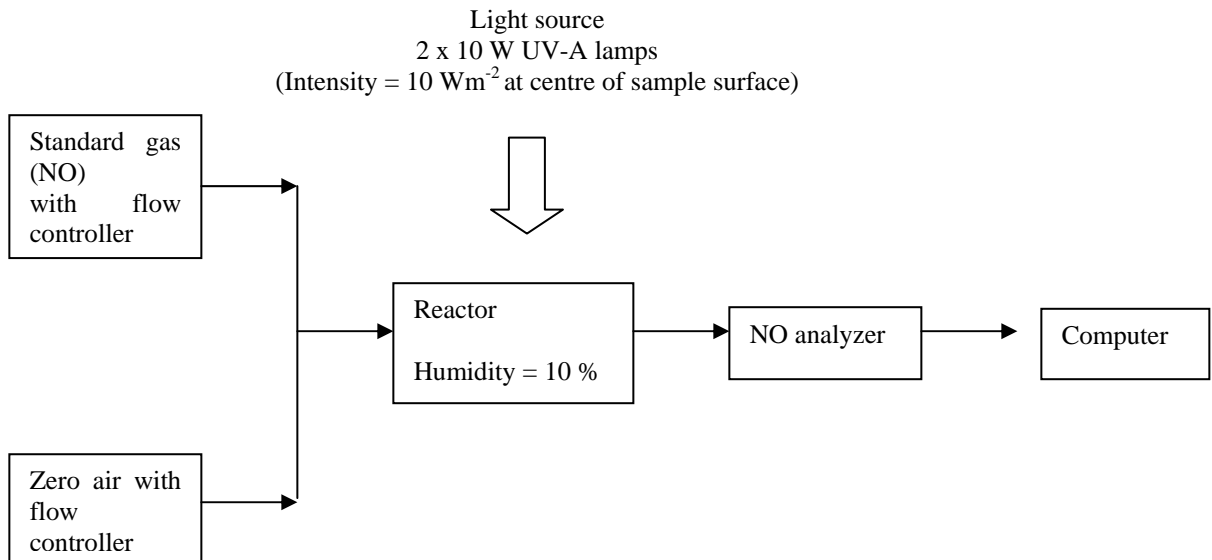


3.5.3.2 Revised procedure

The revised reactor was connected to a supply of standard gas (NO) and a zero air generator. A humidity of 10 % was achieved for the reactor by passing the reactant stream and the zero air stream directly through the reactor. It is possible to achieve a higher humidity by passing the zero air stream through a water bath, but in the revised procedure the humidity was kept at 10 % as at this humidity level observation patterns can be more easily interpreted. Also for comparison purposes this is believed to be reasonable. The gas streams were then adjusted by the flow controllers to achieve an initial NO concentration of 1000 ppb and a flowrate of 6 Lmin^{-1} , these testing conditions in a similar set-up have also been used by Yu [2003] and are believed to be the most ideal from trial. After the inlet and the outlet NO concentrations reached equilibrium (1/2 hour), the UV lamps were turned on to begin the removal process (1 hour). Figure 3.18 shows a schematic diagram of the

experimental set-up. The concentrations of NO and NO₂ were continuously measured by the NO analyzer. To complete the experimental procedure the lamps were then turned off and the supply gas changed to zero air only (1/2 hour).

Figure 3.18 Schematic diagram of the experimental set-up for the revised procedure



3.5.4 Calculation

Figure 3.19 shows the change in NO concentration for a typical test for both the continuous and batch methodology. The amount of NO removed varied depending on the test samples. The amount of NO removed was represented by the area shown. The area was further multiplied by the flow rate and the molecular weight of the testing gas and then divided by 22.4 (an ideal gas occupies 22.4 litres of volume) to derive the amount of NO removed in mg. The amount of NO removed in mg was

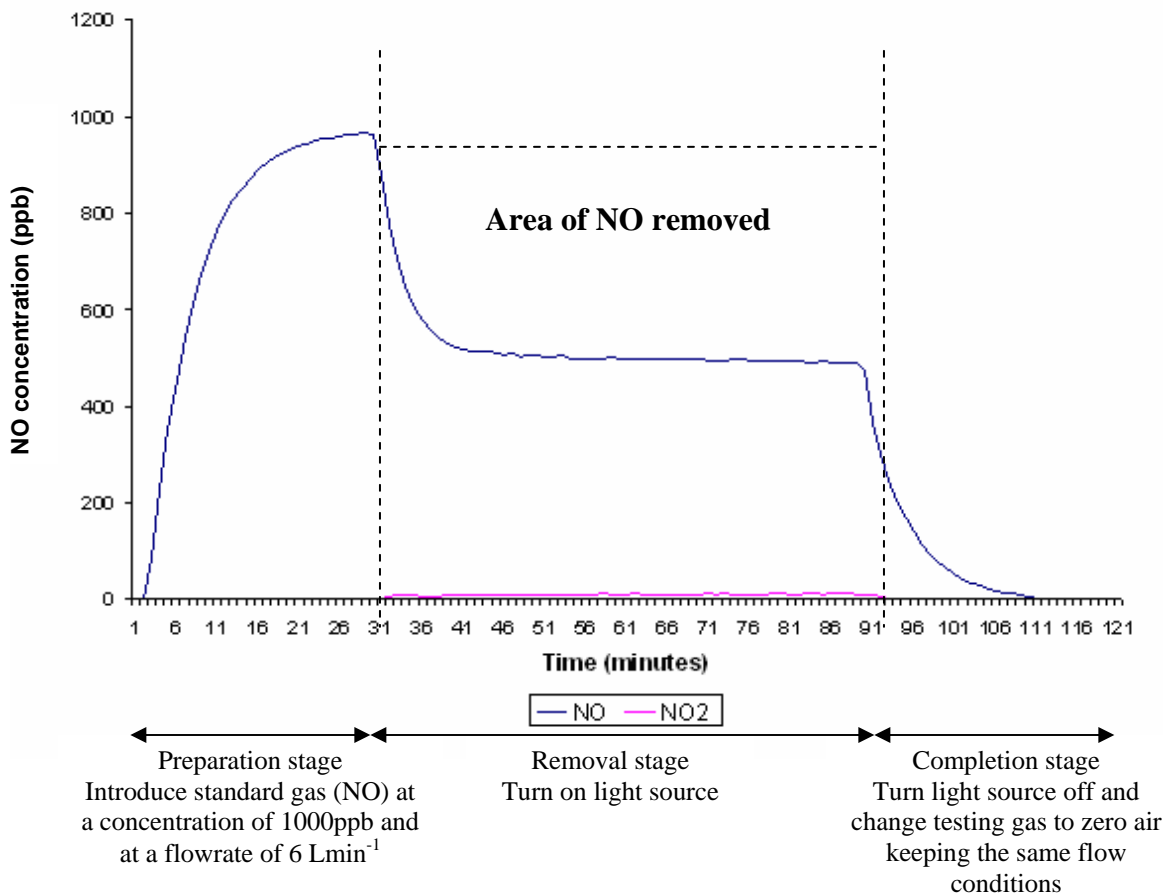
further divided by the removal time in hours and the area of the sample in m^2 to achieve the NO removed in $mg\ hr^{-1}m^2$, which was used to compare the different mix designs of the surface layer. The following equations illustrates the calculation for NO removed ($mg\ hr^{-1}m^2$):

$$\text{NO removed (mg)} = \frac{\text{Area of NO removed (min)} \times \text{NO flow rate (Lmin}^{-1})}{22.4}$$

22.4

$$\text{NO removed (mg}\ hr^{-1}m^2) = \frac{\text{NO removed (mg)}}{\text{Removal time (hr)} \times \text{Sample area (m}^2)}$$

Figure 3.19 Calculation of NO removed



4. Factors affecting the Nitric Oxide photodegradation

4.1 The effect of aggregate material on NO photodegradation

This section investigated the effect on NO photodegradation due to the choice of aggregate material. Materials possessing low density such as FBA were believed to benefit NO photodegradation of the paving blocks when used in the mix design, as these materials were expected to increase the porosity of paving blocks which would effectively increase the surface area available to pollutants, thus allowing further photodegradation.

The compressive strength of the cubes, prepared (with a high cement to aggregate ratio of 1:2) with FBA and RA as the aggregates (Table 3.4), was tested at the curing age of 28 days. The results given in Figure 4.1 indicated that the compressive strength decreased gradually with an increase in the FBA content. This finding was consistent with the results of the density measurement given in Figure 4.2. The density of the mixes decreased linearly with the increase in FBA content.

In the mix design of the surface layers (Table 3.5), FBA was selected due to the assumption that it would be beneficial to NO photodegradation. But the use of FBA alone in the mix design of paving blocks was a concern due to its poorer physical properties such as its low intrinsic strength. Hence a 3:1 FBA to RA ratio was

selected as the mix design for the surface layers as the cube compressive strength of this mix reached 28 MPa which was close to the requirement of local standards concerning paving blocks (30 MPa) [CEDD, 1992].

The surface layers were tested for their ability to remove NO by the batch mode and the continuous mode procedure. For the tests performed in the batch mode, preliminary control runs indicated that, due to the background absorption, the NO concentration within the reactor would drop slightly over the illumination period even when no test specimens were placed inside the reactor. This factor has been accounted for in the calculation of the test results.

Figure 4.1 Compressive strength results of cubes at 28 days testing prepared with FBA and recycled fine aggregate (Table 3.4)

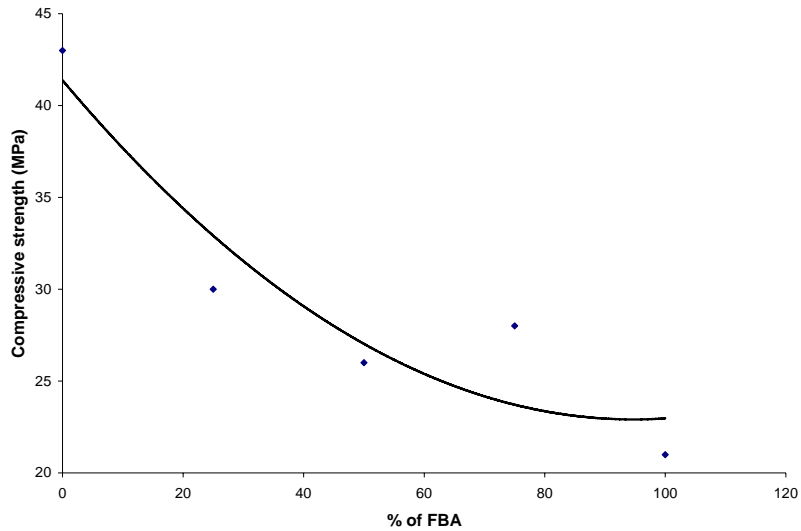


Figure 4.2 Density measurements of cubes at 28 days testing prepared with FBA and recycled fine aggregate (Table 3.4)

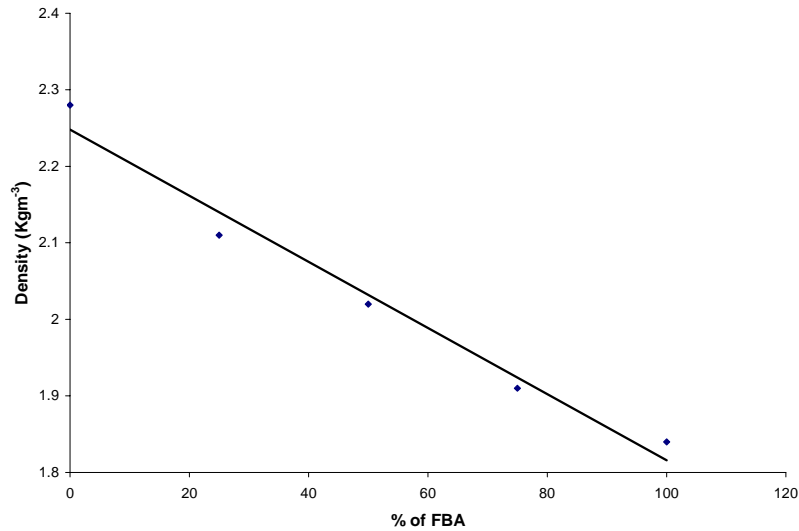


Figure 4.3 shows the results performed in the batch mode as well as in the continuous mode. Each mix notation gives the humidity condition at which the tests were performed, and the number of samples placed inside the reactor at each time in brackets. For example, ‘Batch-25%(3)’ was performed in the batch mode with three specimens at a humidity of 25 %. The removal efficiencies of the 2 % and 4 % TiO₂ specimens were high and similar which indicated the saturation limit should have been reached, so the other specimens at higher TiO₂ percentages were not tested under the same conditions. Instead the same specimens were tested again at a higher humidity of 80 % (notated as ‘Batch-80%(3)’) as it has been reported that the photocatalytical reaction decreases significantly when the relative humidity increases [Ao *et al.*, 2002]. As predicted, the removal abilities of series ‘Batch-80%(3)’ were lower than that of series ‘Batch-25%(3)’. This confirms that humidity

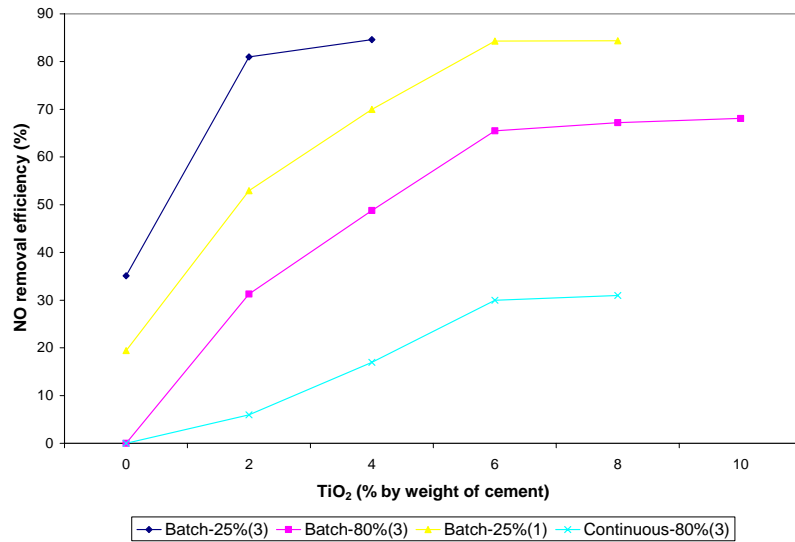
has an important effect on the removal ability. The specimens with 6 % TiO₂ by weight of cement appeared to be the optimum TiO₂ content to be used in the surface layer. The specimens were further tested at a humidity of 25 % again but with one specimen for each test instead of three (notated as 'Batch-25%(1)') for verification. The pattern of the test results achieved in series 'Batch-25%(1)' agreed to those achieved in series 'Batch-80%(3)' hence it can be concluded that 6 % TiO₂ by weight of cement in the surface layer is the optimum content under these testing conditions.

Although water is needed to form the OH radical which is crucial for photocatalysis, no previous research has been found showing the quantity required. But Obee and Brown [1995] showed that the oxidation rate decreases with increasing humidity as excess water will cover the available adsorption areas allowing photocatalysis.

The NO removal abilities of the specimens were also tested in the continuous mode (notated as 'Continuous-80%(3)'). Under the same conditions the specimens tested in the batch mode were approximately double of those tested continuously. NO removal of tests using the batch method showed better ability because for batch testing NO is introduced into the reactor only at the beginning, whereas for continuous testing NO enters the reactor continuously to maintain the concentration level, hence for the same duration continuous testing is dealing with a larger quantity of NO. Therefore continuous testing is not necessarily less efficient at removing NO, just the methods are different so a direct comparison is impossible.

All series showed similar removal patterns. But tests performed continuously were a better representative of the specimens' true removal ability as no loss from the background adsorption would be experienced. Although this factor had been accounted for the tests performed under the batch mode, the results could only represent an approximation.

Figure 4.3 NO removal of specimens tested under the batch and continuous mode (Table 3.5)



FBA, the main component of the aggregate material in the paving blocks, has been relatively new and further studies should be carried out to assess its long-term durability. Therefore, mixes with a larger quantity of RA were designed. Twenty four mixes were prepared with RA, FBA and sand for comparison purposes (Table 3.6).

Amongst the designed mixes, eight were selected and prepared into cubes to test for the compressive strength and density (Table 3.7). The results of these are shown in Figures 4.4 and 4.5 respectively. The compressive strength results show that mixes with 100 % RA achieved the highest values of 41 MPa, followed by the mixes with 100 % sand. The use of FBA in the mixes decreased the strength for both the RA and sand mixes. These results agree with previous findings which showed that increasing the FBA aggregate proportion or replacing either RA or sand by FBA cause a decrease in the compressive strength of the blocks. In addition, mixes of aggregate particle sizes between 300 μm to 2.36 mm were weaker than mixes of aggregate particle sizes below 2.36 mm only. The density measurements for these mixes were consistent with the results of the compressive strength. Although not all the mixes were able to meet the strength requirement prescribed by the international or local standards, they were still tested for NO photodegradation as a larger spectrum of mix designs would be easier to identify the advantages which would aid the photocatalytic ability of the paving blocks.

Figure 4.4 Compressive strength of selected RA and sand mixes (Table 3.7)

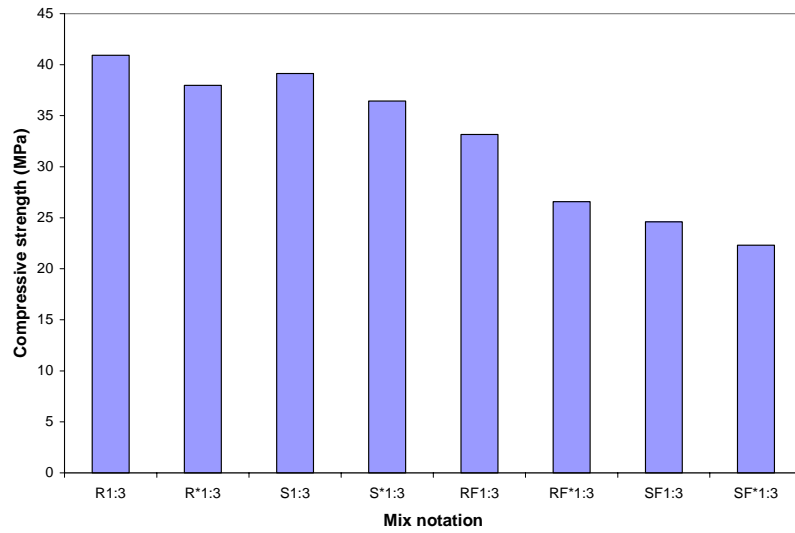
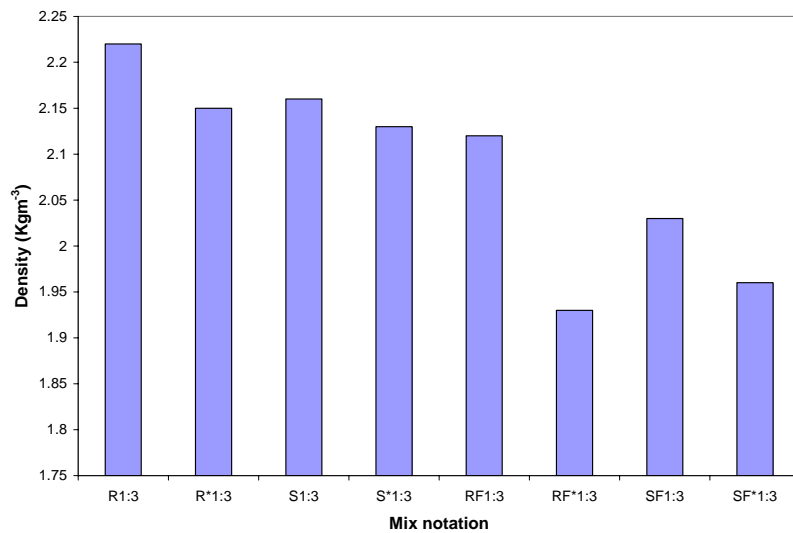


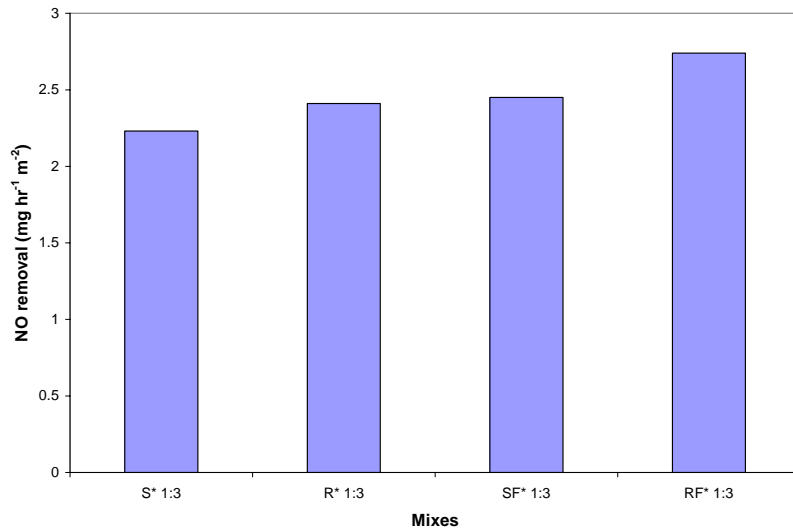
Figure 4.5 Density of selected RA and sand mixes (Table 3.7)



The results of NO photodegradation as shown in Figure 4.6 indicated that the RA mixes achieved much higher NO removal compared to the sand mixes. This was probably due to the porous nature of RA compared to that of sand. The results also

indicated that the NO removal slightly increased when FBA was included in the mix design. This was believed to be due to higher porosity of FBA particles which was exemplified by its relatively low specific density (1877 Kgcm^{-3}) compared to those of sand (2651 Kgcm^{-3}) and RA (2093 Kgcm^{-3}).

Figure 4.6 A comparison of different materials to remove NO at 90 days testing (Table 3.6)

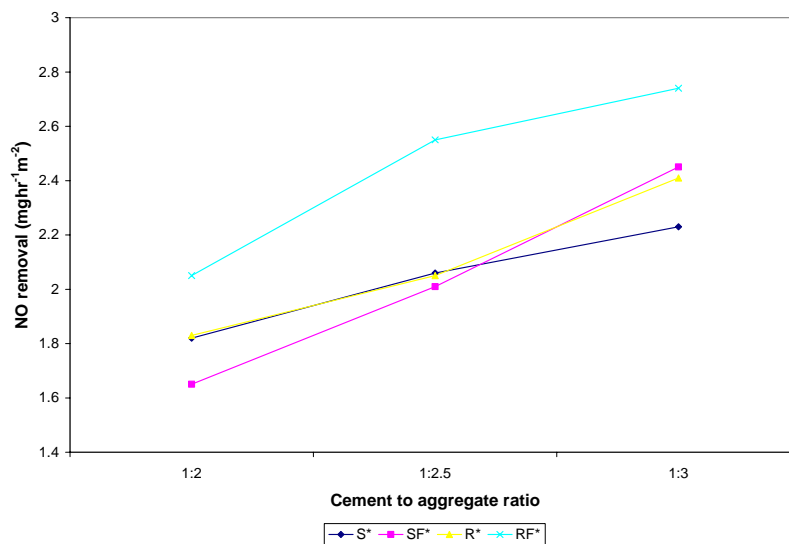


4.2 The effect of cement/aggregate ratio on NO photodegradation

The mixes portrayed in Figure 4.6 have been compared (Figure 4.7) to the same mixes but of other cement to aggregate ratios. The results show that the NO removal increased when the cement content decreased for all mixes. A linear increase in NO removal of approximately 30 % was experienced for specimens when the cement to aggregate ratio dropped from 1:2 to 1:3. The increase in NO removal due to the

change in cement content was a result of the fine particle size of cement grains. Because cement can easily fill up the voids within the specimens, the surface area available for pollutants is reduced. In other words, the surface area could be increased by reducing the cement content, thus allowing efficient removal of pollutants. Although reducing the cement content was favourable towards NO removal, the content designed should consider the necessary strength required for the surface layer. Preliminary studies showed that a minimum cement to aggregate ratio of 1:3 should be used the surface layer.

Figure 4.7 A comparison of NO removal for mixes prepared with different cement contents at 90 days testing (Table 3.6)

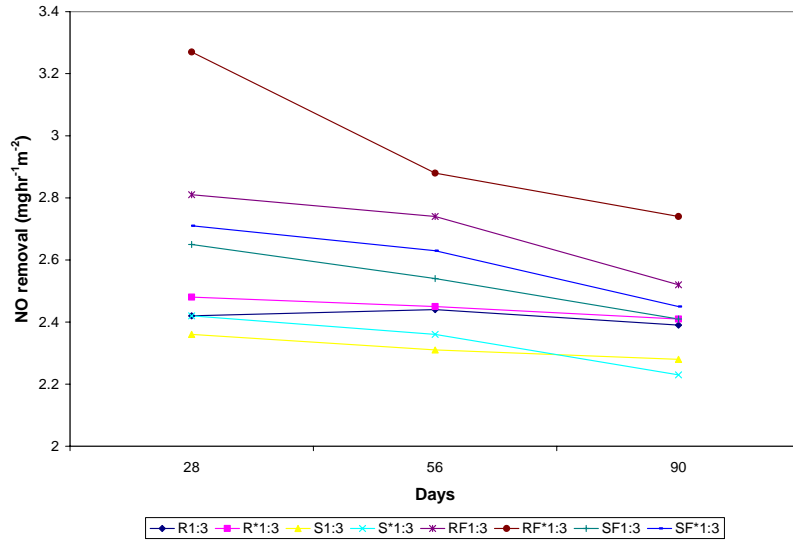


4.3 The effect of curing age on NO photodegradation

All specimens prepared were tested at the curing ages of 28, 56 and 90 days to investigate the influence of curing age on the NO removal of the blocks. The results displayed in Figure 4.8 only show the selected mixes, all with a cement to aggregate ratio of 1:3 which was previously identified as the most appropriate. The results show that NO removal decreased with increasing age from 28 to 90 days by approximately 8 %. This drop was a result of the reduction in the number of active sites due to the closing up of pores as a result of the continuous hydration and carbonization. Lackhoff *et al.* [2003] investigated the possibility of using photocatalyst modified cement samples for the degradation of pollutants and they demonstrated that photocatalytic activity decreased during the ageing of the hardened cement pastes.

The loss of photocatalytic efficiency was due to several factors. They found that the specific area was reduced due to hydration and carbonization hence leading to less active sites. Furthermore, sorptivity decreased due to carbonization as age increased, thus leading to less amount of pollutant adsorbed. In addition, their study was amounted by weight and as weight increased due to carbonization the result was that a smaller amount of particles were available for photocatalysis. Moreover, carbonization can lead to the formation of calcite overgrowth covering and blocking the cement surface.

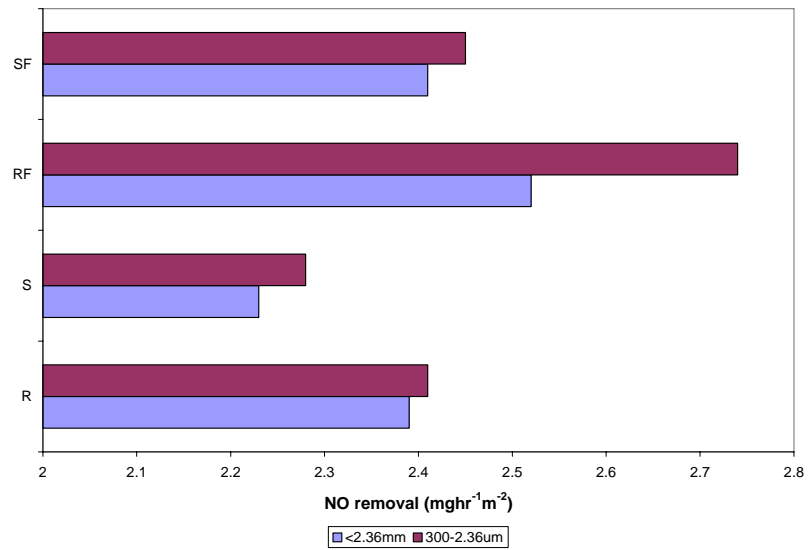
Figure 4.8 NO removal of specimens tested at different curing ages (Table 3.6)



4.4 The effect of particle size of aggregates on NO photodegradation

Specimens prepared with different aggregate sizes was believed to effect their ability to remove NO as altering the particle size distribution of aggregates would effectively change the porosity of the specimens. Specimens were divided into to two groups, ones with all aggregate sizes below 2.36 mm and the other with aggregate sizes only between 300 μm to 2.36 mm. Specimens prepared with aggregate sizes between 300 μm to 2.36 mm were shown to be more porous compared to specimens prepared with aggregate sizes below 2.36 mm. Figure 4.9 shows the specimens tested at 90 days with a cement to aggregate ratio of 1:3. The results indicated that specimens prepared with aggregate sizes between 300 μm and 2.36 mm (the more porous specimens) achieved approximately 4% higher NO removal compared to the other specimens.

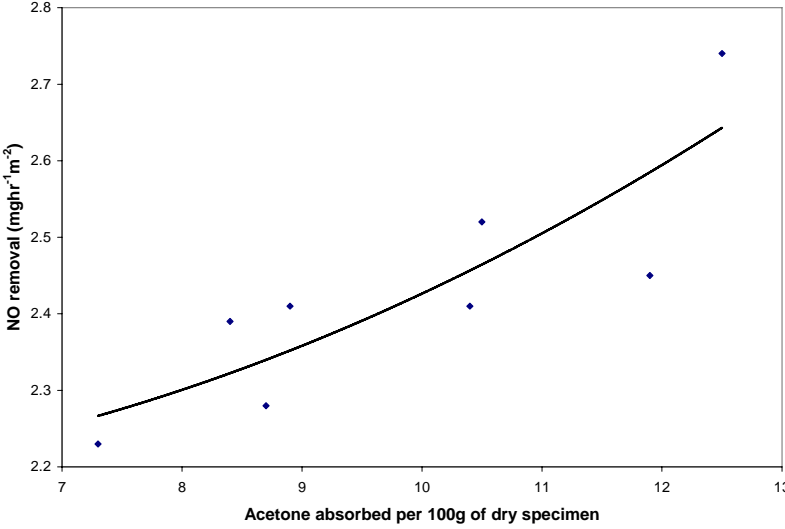
Figure 4.9 NO removal of specimens with different aggregate sizes (Table 3.6)



4.5 The effect of porosity on NO photodegradation

The factors effecting the NO removal discussed in this chapter were all associated with the porosity. The previous results have indicated that high porosity was beneficial to NO removal. In order to justify whether this was true all specimens prepared were measured for their porosity. The amount of acetone absorbed by the dry specimens was used as an indication of the porosity and the measured quantity was represented in grams. Figure 4.10 shows the measured porosity compared to the NO removal of selected mixes. The selected mixes included ones with varying material size, cement content, curing age, TiO₂ source and TiO₂ content, as it was anticipated that material type was not the only factor effecting the change in porosity of the paving blocks. An obvious trend was observed as the NO removal increased with an increase in the porosity.

Figure 4.10 Comparison of NO removal and porosity for selected mixes



5. The effect of incorporating recycled crushed glass cullet

5.1 Characteristics of recycled glass in enabling NO photodegradation

Specimens were prepared with varying aggregate materials (Table 3.8). The results as shown in Figure 5.1 indicated that recycled glass used as aggregates in paving blocks showed better NO removal ability compared to blocks prepared with RA, FBA and sand.

The porosity of the selected mixes was estimated by the amount of acetone absorbed per 100 g of dry sample. The recycled glass mix as shown in Figure 5.2 showed that its ability to absorb acetone was much lower compared to mixes consisting of other aggregate materials. Therefore the higher photoactivity of mixes prepared with glass was not due to porosity, but instead could be due to the high light transmitting characteristic of recycled glass. Light could be carried to a greater depth activating the TiO_2 on the surface as well as within the blocks. This assumption was also supported by Murata *et al.* [2002] when they utilized glass beads in the design of photocatalytical paving blocks in their study.

Figure 5.1 The effect of recycled glass in the mix towards NO photodegradation when compared to other materials at 90 days curing age (Table 3.6 & 3.8)

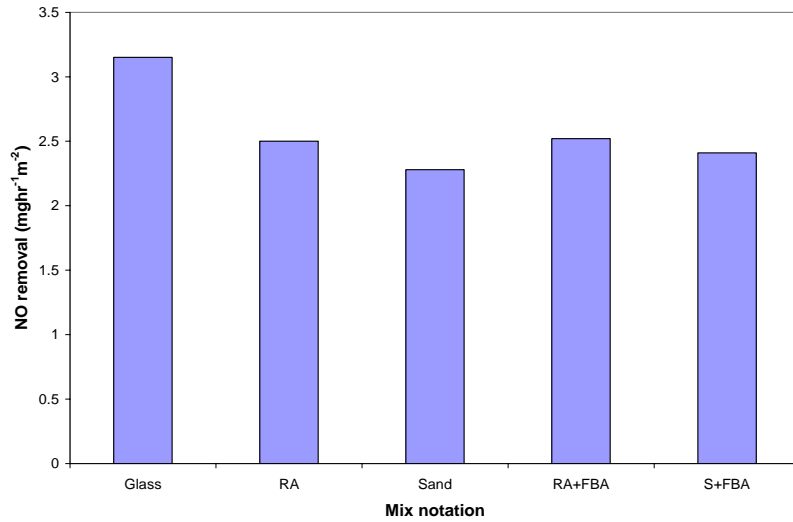
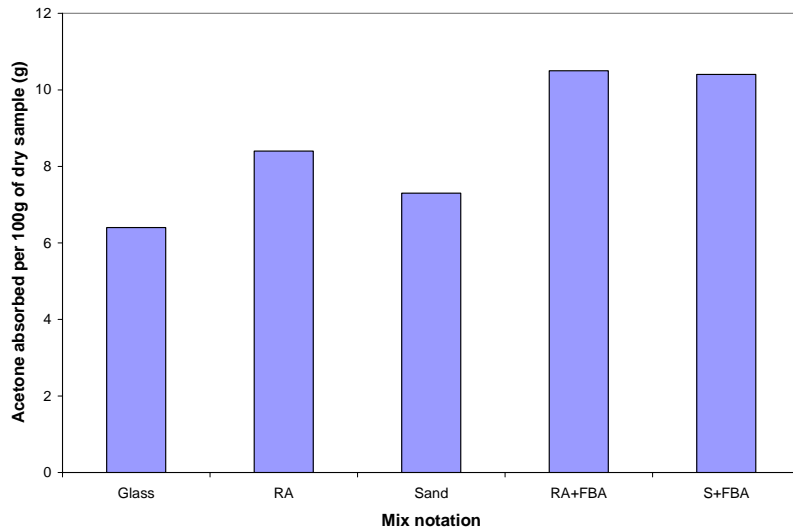


Figure 5.2 The amount of acetone absorbed per 100 g of dry sample for mix with recycled glass and other mixes at 90 days curing age



5.2 Properties of recycled glass mixes

Recycled glass used as aggregate in the paving blocks has shown promising results towards NO photodegradation. Nevertheless, the use of recycled glass was further analyzed for its suitability to be used in paving blocks. Mix designs with recycled glass replacing sand as the aggregate were prepared and tested for their compressive strength and NO removal ability (Table 3.8). Figure 5.3 shows the effect of the incorporation of recycled glass on the compressive strength. The results show that mixes prepared with recycled glass at all replacement levels achieved higher compressive strengths (44 MPa) compared to the mix with 100 % sand as the aggregate (39 MPa). The variation in compressive strengths for all the mixes with recycled glass was small. There was less than 2.5 % difference between recycled glass as 25 % and 100 % replacements of sand.

The same mix designs were prepared for the surface layers and tested for their NO removal ability. The results in Figure 5.4 show that the trend when tested at different curing ages was similar to those results discussed in Chapter 4. At 28 days, NO removal reached the maximum but, thereafter, NO removal decreased gradually until 90 days when the change became negligible. The results also showed quite clearly that NO removal increased with increasing amounts of recycled glass as a substitute of sand. Based on the results, the replacement of sand by recycled glass at 50 % was chosen as the optimal mix since the alkali silica reaction may be a concern

when glass is used in concrete. As a result, a lower replacement level would be a more conservative choice.

Figure 5.3 Compressive strength of mixes when recycled glass replaces sand as the aggregate in the mix design at 28 days curing age (Table 3.8)

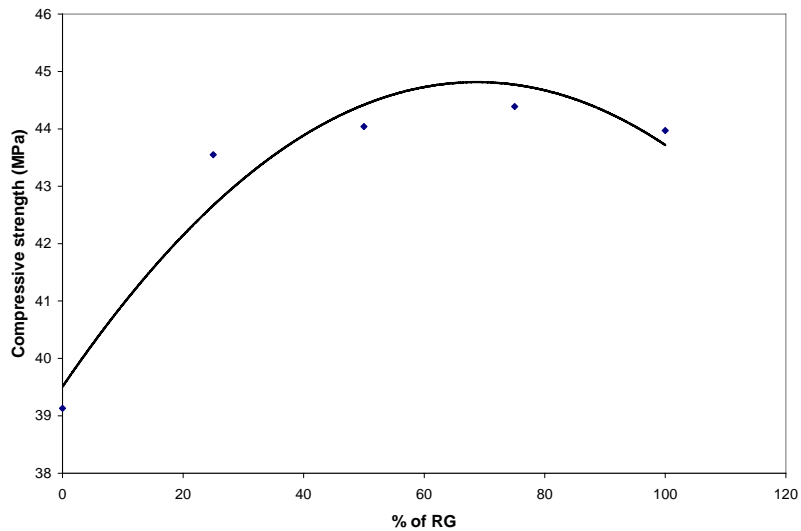
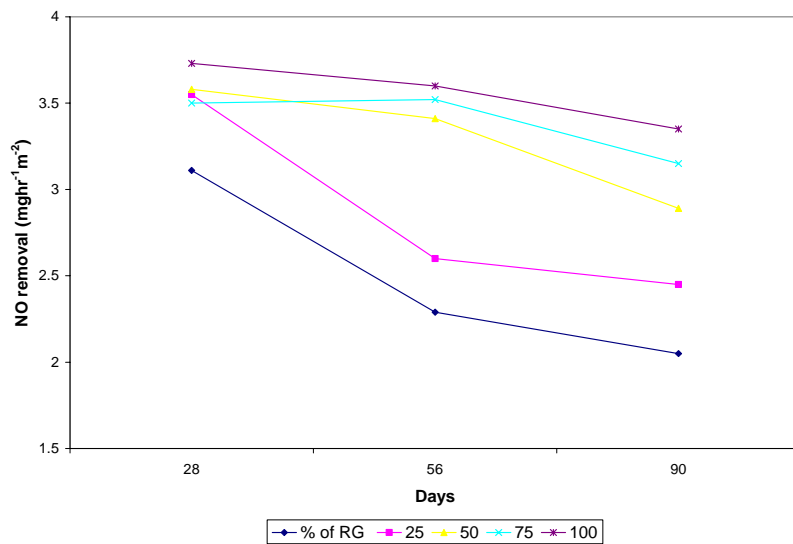


Figure 5.4 NO removal of mixes with different proportions of recycled glass replacing sand as the aggregate at different curing ages (Table 3.8)



5.3 Enhancing NO photodegradation of paving blocks containing recycled glass

Crushed transparent glass bottles sourced from a local sauce manufacturer has been used as the recycled glass. In order to further enhance NO photodegradation of the paving blocks, three other types of glass were also selected to compare their performance with the recycled glass sourced from the sauce manufacturer. These included another transparent glass sourced from crushed milk bottles (denoted by 'T'), and green and brown coloured glass obtained from crushed beverage bottles (denoted by 'G' and 'B' respectively).

Specimens prepared with different types of glass were tested for their compressive strength and NO removal ability (Table 3.9). Figure 5.5 shows the compressive strengths of the various mixes. The results indicated that the mix containing the original transparent glass had a slightly higher compressive strength.

Although coloured glass in the mix design might not be as efficient with respect to pollutant removal compared to transparent glass as some of the light maybe blocked by the glass color, Figure 5.6 shows that this was not a valid assumption. Despite the expected NO removal was less for samples with either the green or the brown colored glass, the NO removal achieved by the transparent glass from milk bottles was lower than the original transparent glass samples by approximately 20 %. However, all mixes prepared with glass showed higher NO removal compared to the

pure sand mix. The difference in the performance of different types of glass mix cannot be solely explained by the glass colour.

It is possible that the overall particle grading of the paving block materials also influenced the performance. The variation in the particle grading could be large as different types of recycled glass were either crushed by hand in the laboratory or already crushed by the glass collectors using different machinery or methods depending on the source. To eliminate a wide variation of grading for the glass, the same method and machinery for crushing the glass into cullets should be utilized in the future. Further research is needed to quantify these factors. Figure 5.7 illustrates the possible paths of light rays for a section of a paving block prepared with recycled glass while Figure 5.8 illustrates a section prepared with other materials as a comparison.

Figure 5.5 Compressive strength of mixes with different sources of recycled glass at 28 days curing age (Table 3.9)

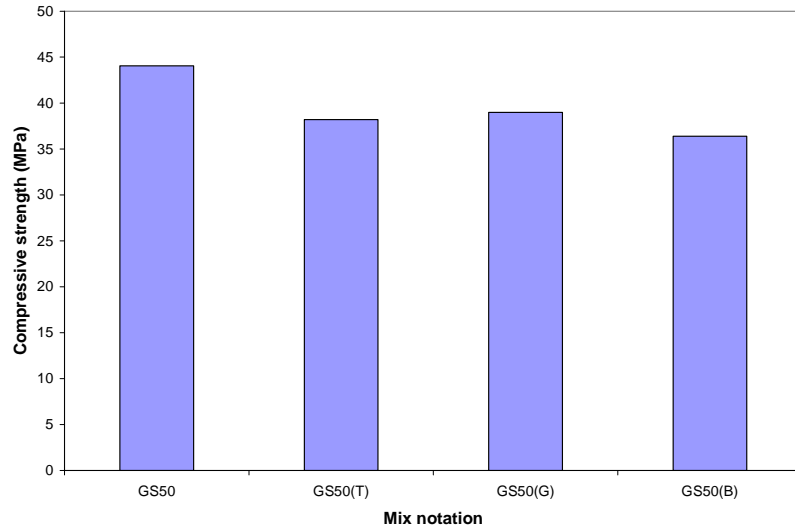


Figure 5.6 NO removal of mixes with different sources of recycled glass at various curing ages (Table 3.9)

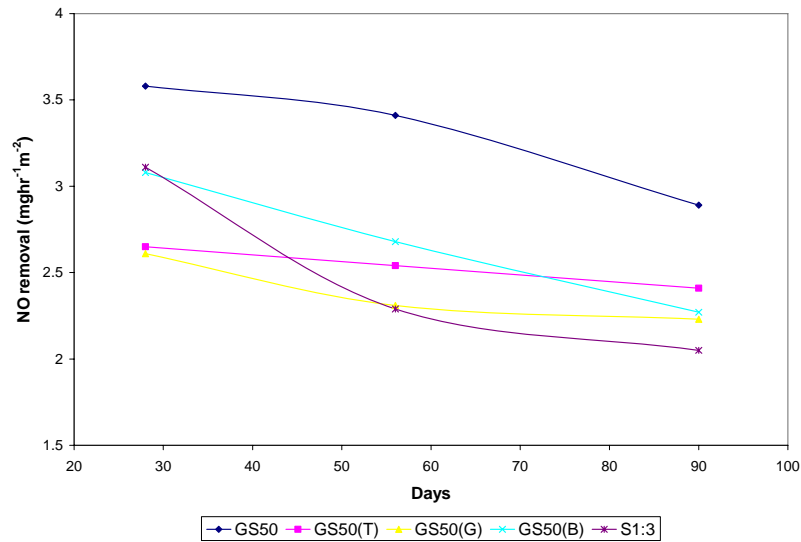


Figure 5.7 Possible paths of light rays for a section of a paving block prepared with recycled glass

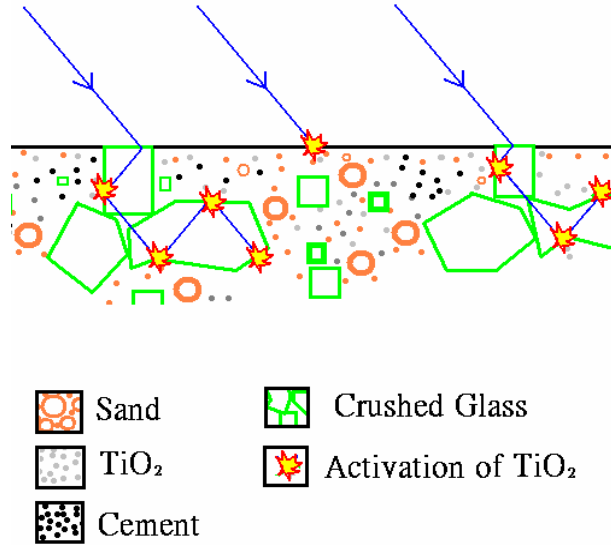
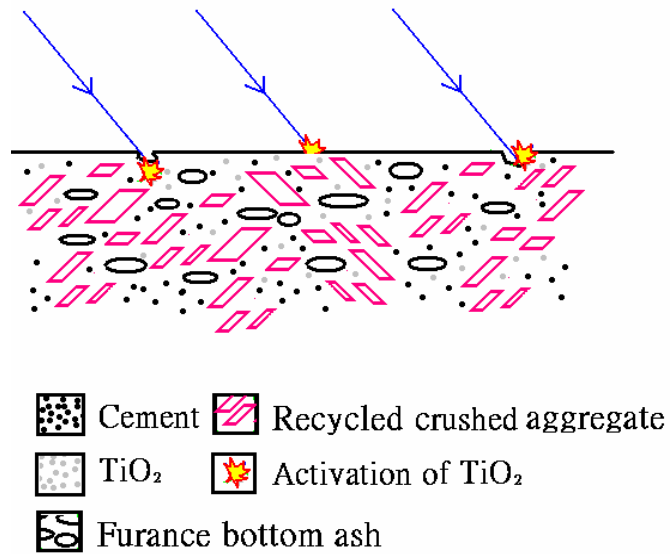


Figure 5.8 Possible paths of light rays for a section of a paving block prepared with recycled fine aggregates



5.4 Prevention of the paving blocks from alkali silica reaction (ASR)

Glass cullet possesses obvious advantages such as low water absorption and high strength, but there is still a potential problem since it is well known that glass would induce alkali silica reaction (ASR) when used as the aggregates in cement-based construction materials. The optimum mix design was then further analyzed for the potential ASR reaction using the mortar bar test method. Two types of pozzolanic materials, Metakaolin (MK) and pulverized fly ash (PFA) which are known to be able to control ASR [Aquino *et al.*, 2001], were separately added at different percentages by weight of the aggregate in the mix design to evaluate its ability to mitigate the potential expansive reaction (Table 3.10).

Figures 5.9 and 5.10 show the expansion of mortar bars prepared with MK and PFA, respectively. According to the international standards [ASTM, 2001], the expansion of mortar bars should not exceed 0.1 % after 14 days of testing. It is shown that all the mixes prepared were able to meet this requirement with and without the addition of MK or PFA. Nevertheless, MK and PFA were able to reduce the expansion as a result of ASR.

The mixes were further tested to analyze if the addition of MK or PFA would affect the ability of paving blocks to photodegrade NO. Figure 5.11 shows that the addition of both materials lowered NO photodegradation, with the effect of PFA being more extreme. The difference between the different percentage additions of

each was minimal. The use of MK would be the more desirable option in this situation as the effects were less obvious compared to PFA.

Figure 5.9 Expansion of mortar bars with MK addition by cement weight at 2.5 %, 5 % and 10 % (Table 3.10)

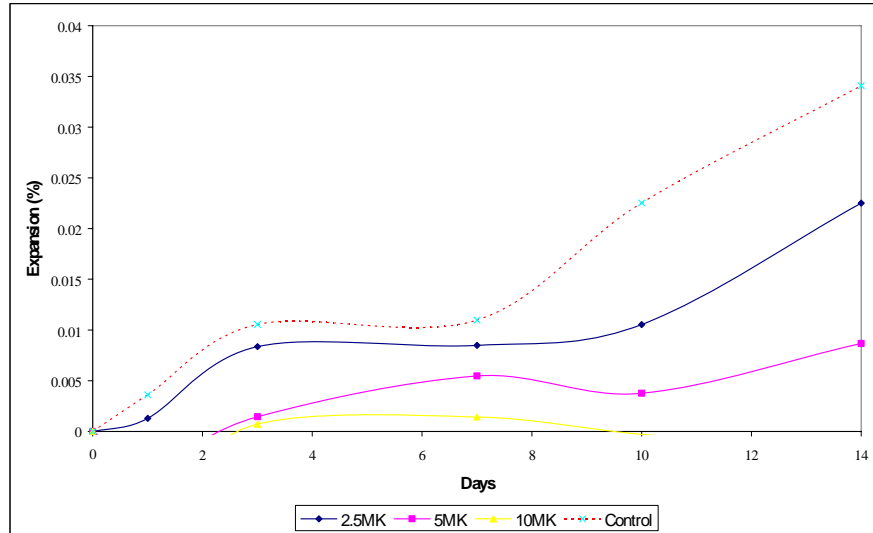


Figure 5.10 Expansion of mortar bars with PFA addition by cement weight at 2.5 %, 5 % and 10 % (Table 3.10)

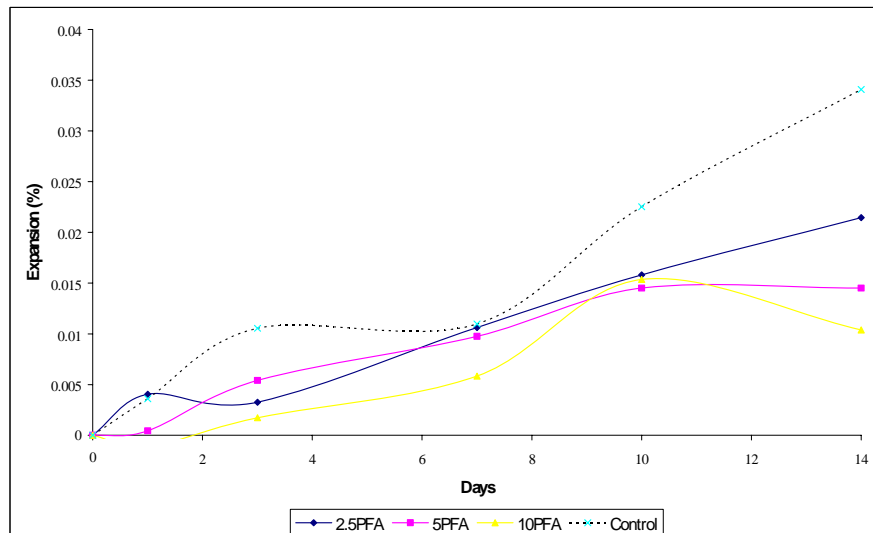
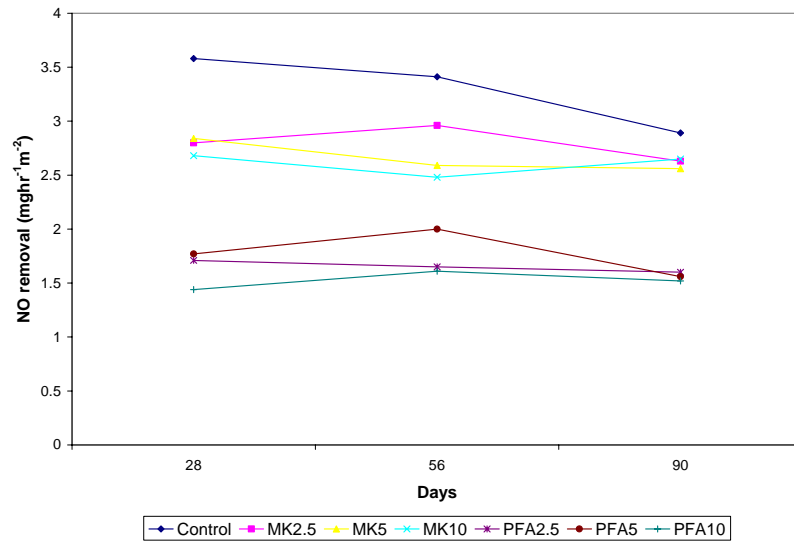


Figure 5.11 NO removal of mixes with either MK or PFA addition by cement weight at 0 %, 2.5 %, 5 % and 10 % (Table 3.10)



6. Enhancing the ability of titanium dioxide for nitric oxide photodegradation

6.1 The effect of increasing TiO₂ content of the paving blocks

One of the focal points of this research project was to efficiently incorporate TiO₂ within the mix design of the blocks to allow the removal of pollutants. Hence it was important to consider options which would improve this characteristic. Nevertheless, it was important to investigate the effect that TiO₂ might have on the physical properties of the blocks and whether this effect would be beneficial or disadvantageous to the blocks. The design of the photocatalytic block considers two main factors: 1) the ability of TiO₂ for NO photodegradation and 2) the physical properties of the block which determine its appropriateness for pavement use. The physical properties should not suffer as a result of enhancing the photocatalyst ability.

A mix design was selected from the results achieved in Chapters 4 and 5 and was used to prepare specimens with the TiO₂ content ranging from 0 % to 10 % at 2 % intervals (Table 3.11). The compressive strength and density were determined for the prepared blocks as shown in Figures 6.1 and 6.2 respectively. The results indicated that the TiO₂ content had a negligible influence on both the strength and density.

Specimens prepared with the same mix designs were further studied to analyze the effect caused to NO photodegradation when increasing the TiO₂ content. The results as shown in Figure 6.3 indicated that there was a definite increase in NO removal for specimens with an increase in the TiO₂ content. At 90 days, NO removal increased from 2.56 mg hr⁻¹ m⁻² for specimens with 2 % TiO₂ to 4.01 mg hr⁻¹ m⁻² for specimens with 10 % TiO₂. The corresponding increase was 57 %. Although NO removal increases as the TiO₂ content increases up to 10 % by weight of the whole mix, the effectiveness of the use of higher TiO₂ content on the NO removal needs to be verified by future studies.

Figure 6.1 The effect of compressive strength with increasing TiO₂ content (Table 3.11)

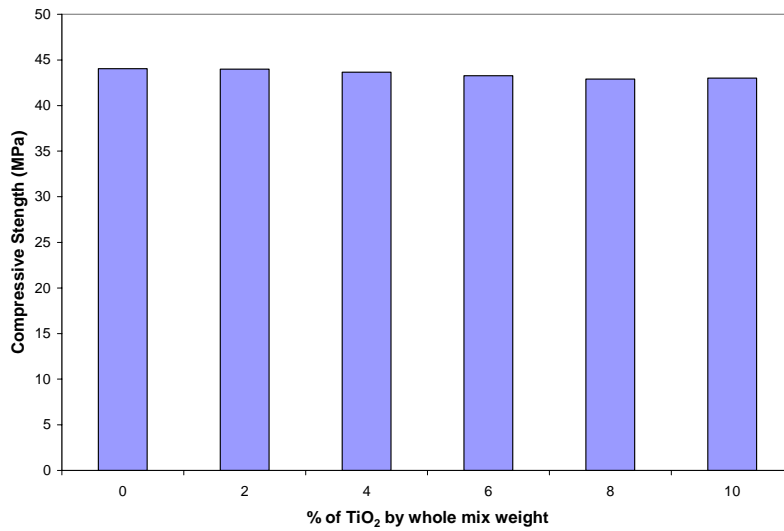


Figure 6.2 The effect of density with increasing TiO₂ content (Table 3.11)

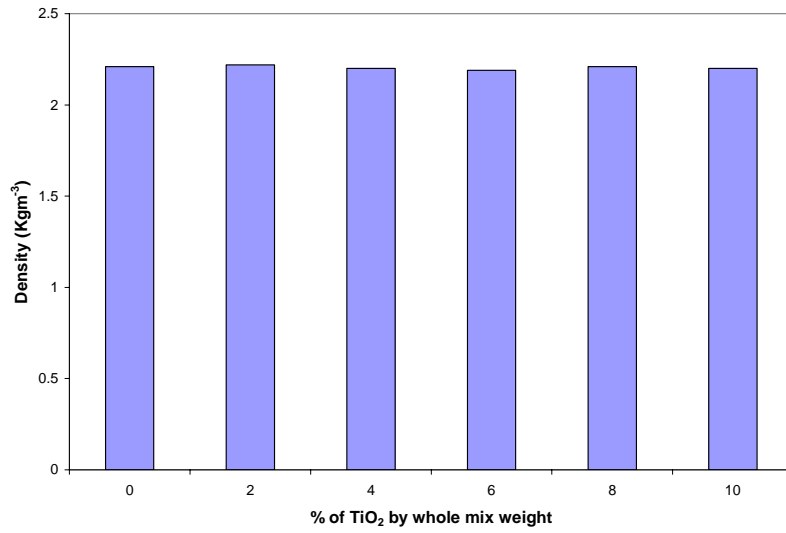
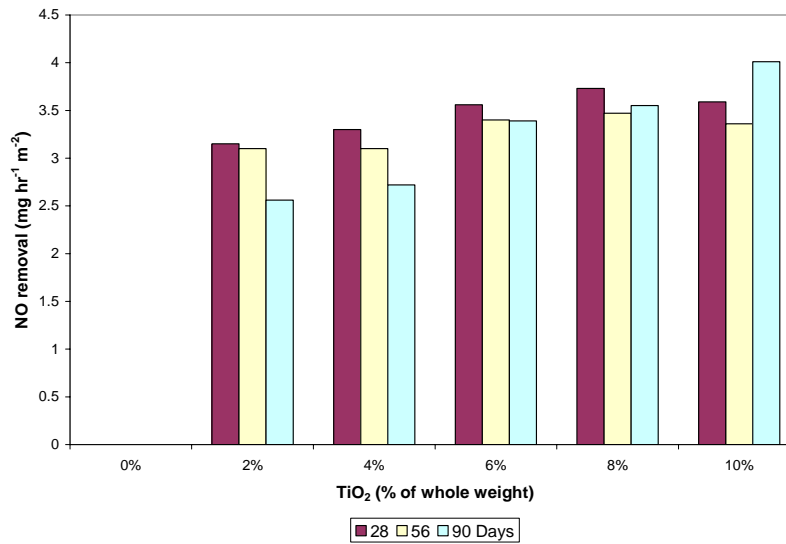


Figure 6.3 The effect of NO removal at different TiO₂ contents (Table 3.11)



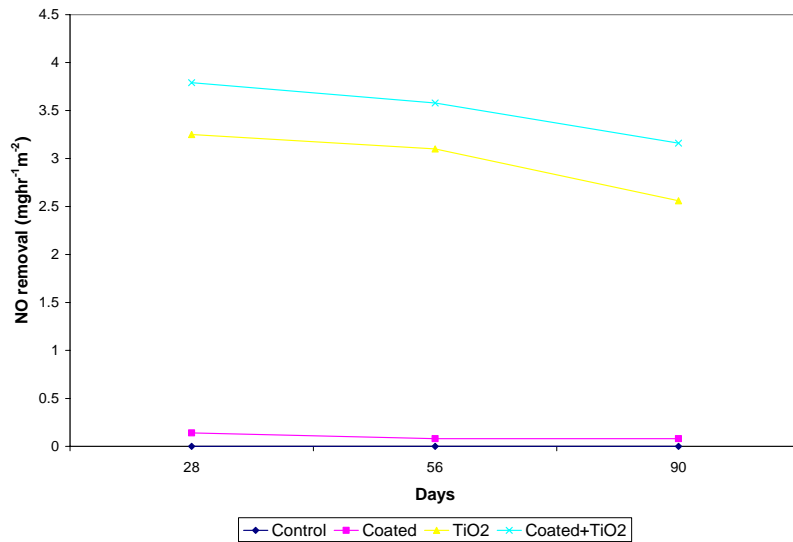
6.2 Incorporating TiO₂ coated glass cullets within the mix design of paving blocks

The use of commercially available TiO₂ powder in the mix design of the paving blocks has shown positive results for NO photodegradation. In order to improve this ability, the recycled glass was coated with the assistance of The Chinese University to analyze the effect when used in the mix design replacing the ordinary recycled glass (section 3.2.3).

Four mixes were prepared, two with the coated glass and the other two without (Table 3.12). The ‘control’ mix was prepared with the original recycled glass and no TiO₂ powder. The ‘coated’ mix was prepared with the coated recycled glass replacing the original recycled glass and no TiO₂ powder. The ‘TiO₂’ mix was prepared with the original recycled glass and TiO₂ powder and the ‘coated+TiO₂’ mix was prepared with the coated recycled glass replacing the original recycled glass as well as the use of the TiO₂ powder. The NO removal results of these mixes as shown in Figure 6.4 indicate that the ‘coated+TiO₂’ mix was the most efficient in removing NO. This revealed that the replacement of the original recycled glass by coated glass was beneficial. The improvement was 23 % compared to the ‘TiO₂’ mix at 90 days. The ‘coated’ mix alone was less efficient at 90 days testing and a removal rate of 0.08 mg hr⁻¹ m⁻² was achieved which was 97 % less than the ‘TiO₂’ mix. The poor performance achieved was very much due to the low quantity of photocatalyst used during the coating preparation. The ‘control’ mix showed no

removal ability at all the test ages. ‘Coated+TiO₂’ was therefore the best mix in terms of NO photodegradation ability, but more analysis on the feasibility of using coated glass is required as the production is a lot more costly.

Figure 6.4 NO removal of specimens with and without TiO₂ coated glass cullets (Table 3.12)



6.3 A comparison of different sources of TiO₂

Three types of commercially available TiO₂ powders were compared. Specimens of the same mix design were produced in which the only the source of TiO₂ was varied (Table 3.13). The TiO₂ powders chosen included P-25 from Degussa Company which is a combination of anatase and rutile forms. It was chosen because of its high purity and accurate specifications and has been used throughout this research. An anatase form and a rutile form of TiO₂, both sourced from Ke Xiang Company, were

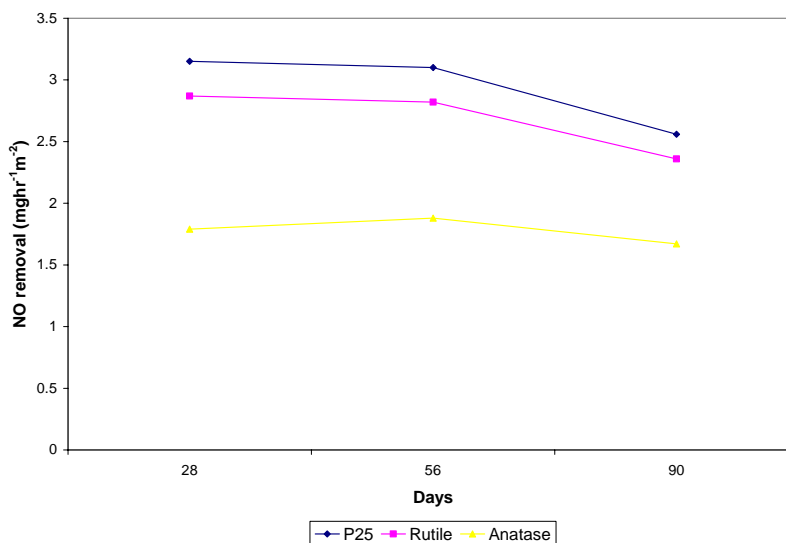
also chosen due to their low prices compared to that of P-25 (Table 6.1). The specimens were subsequently tested for NO removal. The results as shown in Figure 6.5 indicate that, at all test ages, P-25 showed the best removal ability, followed by the rutile form of TiO₂ and the anatase form of TiO₂. Indeed, the NO removal for P-25 and the rutile form of TiO₂ was very close. At 90 days, the NO removal of P-25 was higher by only 8 % compared to the removal of the rutile form. On the other hand the NO removal for the anatase form of TiO₂ was 53 % lower compared to that of P-25.

Table 6.1 Price comparison of TiO₂

Source of TiO ₂	Price per Kg (HK\$)	Price per block* (HK\$)
Degussa P25	300	1.50
Ke Xiang Rutile	16.50	0.08
Ke Xiang Anatase	10.80	0.05

*TiO₂ at 2 % of the whole surface layer weight

Figure 6.5 NO removal of specimens containing different sources of TiO₂ (Table 3.13)



The rutile form of TiO₂ performed better photocatalytically when used in the mix design of the paving blocks compared to the anatase form despite the anatase form is generally believed to be more photoactive [Dehn *et al.*, 2004]. It has been reported in a previous study that the rutile form can perform more actively or as well as the anatase form in certain reactions. [Domenech, 1992]. In addition Deng *et al.* [2002] showed that the activities of pure anatase TiO₂ and pure rutile TiO₂ catalysts with almost the same surface area and crystal size for photocatalytic oxidation of hexane were similar.

The TiO₂ powder Degussa P-25 consists of both the anatase and rutile forms at a ratio of 70:30. P-25 has often been considered as one of the best and most frequently used TiO₂ photocatalysts. Ohno *et al.* [2001] explained the excellent

ability of P-25 was due to a synergy effect as a result of the anatase and rutile particles in contact. Anatase and rutile TiO₂ particles exist separately by forming their agglomerates in P-25. Therefore electron transfer was feasible via the agglomerates which as a result lead to high activity of P-25.

There are a wide range of factors which could possibly affect the activity of TiO₂ used in this study. These could include the crystalline forms, surface area, particle size, porosity, surface acidity and density of surface adsorbed water and hydroxyl groups [Wu *et al.*, 2004]. Amongst these the particle size was one of the easier factors to determine due to the available apparatus. Hence the three TiO₂ powders were tested for their particle size distribution. The results (Figure 3.1) show that the particle size decreased in the order of P-25, followed by the rutile form and then the anatase form. Hence the larger TiO₂ particles were more beneficial to the photocatalytic activity of the paving blocks. Small TiO₂ particles have often been believed to benefit photoactivity due to increasing the surface area when compared to large particles of the same weight, but in the case of TiO₂ powder used in the paving blocks this may not be true. The results indicated that smaller particles are not as photoactive in the paving blocks, which could be attributed to the presence of other materials such as the cement in the paving blocks which covered the TiO₂ particles. Further research is required to conclude this finding.

The TiO₂ powders were further analysed for their chemical composition using x-ray diffraction patterns. The results in Figure 3.2 show that P25 possessed TiO₂ in the

forms of anatase and rutile. Whereas the anatase form of TiO₂ contained only the anatase form and the rutile form of TiO₂ contained only the rutile form.

Similar to P-25 the anatase and rutile forms of TiO₂ were both tested for NO removal when the TiO₂ content in the paving blocks was increased. Figures 6.6 and 6.7 show the effect of NO removal at different TiO₂ contents. Both sets of results followed the same trend as P-25, with a steady increase in NO removal when the TiO₂ content was increased up to 10 % by weight of the whole mix. For the anatase form of TiO₂, an increase of 39 % was experienced from 1.67 mg hr⁻¹ m⁻² to 2.32 mg hr⁻¹ m⁻² when the TiO₂ content increased from 2 to 10 % at 90 days respectively. For the rutile form of TiO₂, an increase of 49 % was experienced from 2.36 mg hr⁻¹ m⁻² to 3.52 mg hr⁻¹ m⁻² when the TiO₂ content increased from 2 to 10 %.

Figure 6.6 NO removal at different TiO₂ (anatase) contents (Table 3.14)

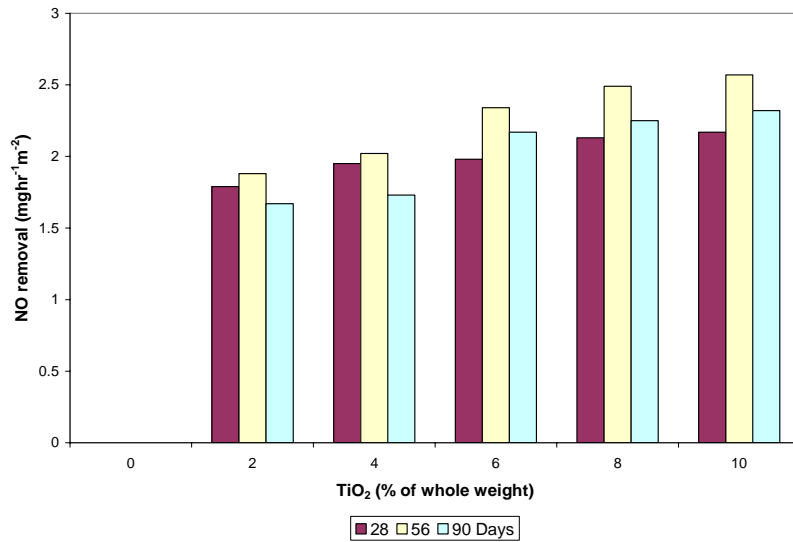
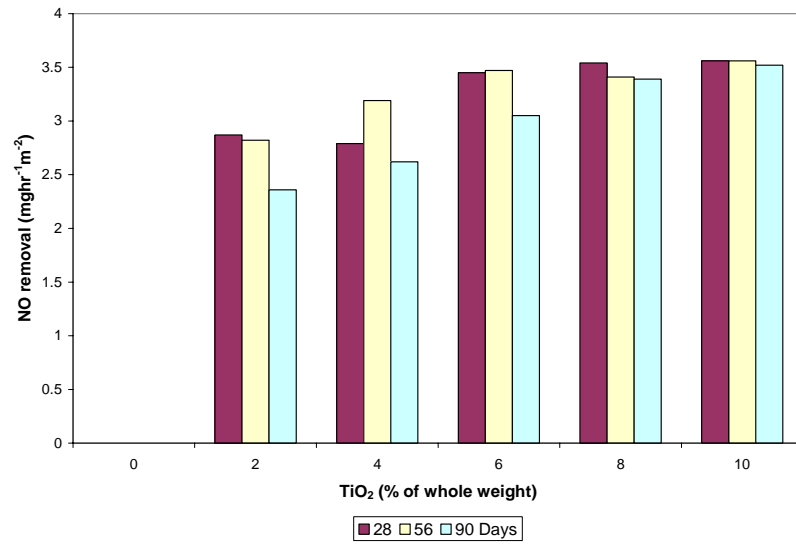


Figure 6.7 NO removal at different TiO₂ (rutile) contents (Table 3.14)



7. Field trial

To determine the deactivation and regeneration properties of the photocatalytic paving block when used in field conditions, mix designs were selected for a plant trial production. This chapter reports the mix designs selected for the trial, the manufacturing process of the blocks, the physical properties of the blocks, the techniques used to monitor the effect on the air quality using these paving blocks and also the analysis of the block durability after some preliminary usage and exposure in a real life environment.

7.1 Mix proportions of paving blocks

An optimum surface layer mix design from the obtained results was selected for block manufacturing in a factory. The selection was based on the physical properties, the ability to remove NO, cost consideration and practicability. Three types of paving blocks were manufactured in the factory. They have been identified as B-1, B-2 and B-3. B-1 and B-2 both comprised two layers, a base layer and a surface layer which was consisted of the photocatalyst. On the other hand, B-3 comprised only the surface layer. The mix design for the surface layer was selected based on previous results and was the same for B-1, B-2 and B-3 (Table 7.1). The cement to aggregate ratio was 1:3, with the aggregate proportion consisting of 50 %

recycled glass and 50 % sand. P-25 TiO₂, Metakaolin and a blue pigment were added at 8, 5 and 2 % by weight of cement, respectively.

The two primary factors affecting the strength of paving blocks are the aggregate grading and cement to aggregate ratio based on this the base layer was designed according to past experience as well as the test results of the cube compressive strengths in Chapters 4-6. The base layers of B-1 and B-2 differed by the choice of aggregates used. B-1 only used the natural aggregate whereas B-2 only used recycled aggregate material. The base layer of B-1 (Table 7.2) utilized a cement to aggregate ratio of 1:3, with the aggregate proportion consisting of 35 % natural aggregate of 10 mm nominal size and 65 % coarse sand of <5 mm. The base layer of B-2 utilized a cement to aggregate ratio of 1:3, with the aggregate proportion consisting of 35 % recycled coarse aggregate of 10 mm nominal size and 65 % recycled fine aggregate of <5 mm.

Table 7.1 Mix design for surface layer

Mix notation	Materials (Kg)						
	Cement	Fine river sand (2.36mm)	Recycled glass (2.36mm)	P-25 TiO ₂	Metakaolin	Pigment	
Surface layer	1	1.5	1.5	0.08	0.05	0.02	

Table 7.2 Mix design for base layer

Mix notation	Materials (Kg)				
	Cement	Natural aggregate (10mm)	Coarse sand (<5mm)	Recycled coarse aggregate (10mm)	Recycled fine aggregate (<5mm)
B-1 Base layer	1	1.05	1.95	-	-
B-2 Base layer	1	-	-	1.05	1.95

7.2 Pilot manufacture of paving blocks

The blocks were manufactured according to the determined previous mix designs (Tables 7.1 and 7.2) with the assistance of a local block manufacturer. The production sequence is shown in Figures 7.1-7.4. The dimensions of the final product were 100 x 200 x 60 mm. For B-1 and B-2 the base layer was about 55 mm and the surface layer was about 5 mm.

Figure 7.1 Materials poured into to mixer chute



Figure 7.2 Machinery



Figure 7.3 Block manufacture



Figure 7.4 The final products



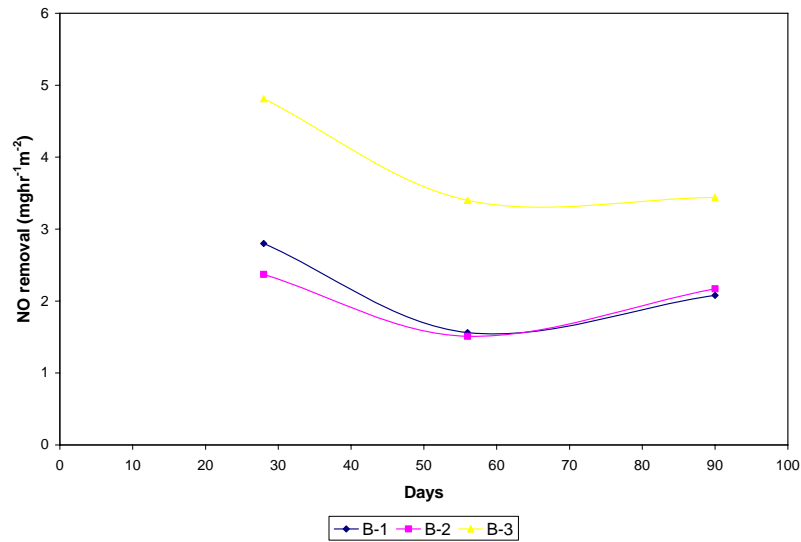
7.3 Properties of the photocatalytical paving blocks

7.3.1 NO photodegradation

The produced paving blocks were taken back to the Hong Kong Polytechnic University laboratory and tested for the ability to photodegrade NO at 28, 56 and 90 days. The NO removal of the samples, were tested at 28, 56 and 90 days to compare with the physical properties of the samples which were also tested at these dates. These dates coincide with previous studies on concrete technology which analyze the trend in cement hydration. At 90 days testing cement hydration is almost complete. Whereas many physical properties of paving blocks are tested at 28 days according to the British Standards and the Hong Kong General Specifications. In addition 56 days was also identified as it marks the in between of 28 and 90 days.

Similar to previous results achieved, Figure 7.5 shows that NO removal was the highest at 28 days. However, the NO removal after 90 days was the better representative in the long-term. The results for B-1 and B-2 were very similar. As for B-3, comprised only the surface layer, the results show that the NO removal performance was much better. As the mix design for B-3 was identical to the surface layer of B-1 and B-2, it was possible that activation of the TiO₂ took place at a depth of more than 5 mm (5 mm was the thickness of the surface layers for B-1 and B-2).

Figure 7.5 NO removal of B-1, B-2 and B-3 and different curing ages (Tables 7.1 and 7.2)



7.3.2 Physical properties

Tests according to CEDD [1992], BS 6717 [1993] and BS 6717 [2001] were performed on the paving blocks and their physical properties were derived. The results given in Table 7.3 show that the paving blocks were able to satisfy most of the standard requirements. B-2 achieved a cold water absorption of 8.04 % which was higher than the requirement but for further studies it is worth considering the use of recycled glass in the base layer to help lower this value.

Table 7.3 Physical properties of the paving blocks

Mix notation	Compressive strength (MPa) (>30MPa)	Density (Kgm ⁻³)	Skid resistance (BPN) (>45 BPN)	Abrasion (mm) (<23mm)	Cold water absorption (%) (<6%)
B-1	57	2270	111	20.24	5.32
B-2	61	2310	105	20.17	8.04

7.4 Site trial

Only B-1 and B-2 were used in the site trial as the physical properties of B-3 were not satisfactory. The site location chosen for laying the paving blocks was based on convenience for air monitoring and level of usage. The stretch of pavement tested was located in The Hong Kong Polytechnic University Campus (Figure 7.6 and 7.8). The location receives an appropriate amount of usage from pedestrians and the amount of air pollution is relatively high as the campus is located in an urban environment surrounded by the harbour tunnel crossing as well as some major roadways (Figure 7.9).

Figure 7.6 Distant view of site location



Figure 7.7 Photocatalytic pavement



Figure 7.8 Close-up of photocatalytic pavement and original pavement



Figure 7.9 Map of site location [Centamap, 2004]



7.5 Air monitoring of paving blocks

The air quality of the site location was continuously monitored for differences in pollutant concentration between the pavement using the photocatalytic block and the original block without photocatalytic properties. Air monitoring was carried out by collecting air bags from the selected points using a hand held pump which collected air at a rate of 2 Lmin^{-1} . A total of six collection points were selected where three were at the photocatalytic pavement and the rest were at the non-photocatalytic pavement (Figure 7.10). At each point air bags (Figure 7.11) were collected at ground level and at breathing zone. Table 7.4 shows the weather conditions recorded when monitoring took place, and Table 7.5 shows the actual data of pollutant concentrations collected from the monitoring since the paving blocks were

laid. As the photocatalytic paving was laid next to the original paving there should be no differences in environmental or topographic conditions.

From the collected data the percentage drop in concentration of the monitored pollutants due to the photocatalytic paving was calculated (Table 7.6). Monitoring of the air quality is an on-going process in order to observe the possible differences over time, but the initial findings from the first 6 months have shown that the photocatalytic paving blocks do have an effect towards the surrounding air quality. Using the photocatalytic paving, NO concentrations at ground level were reduced by an average of 12 %. A 8 % NO reduction was achieved using the photocatalytic paving at breathing zone. The observations indicated that NO was the only pollutant that showed an obvious difference, the other pollutants which were also monitored included NO₂, CO and SO₂, showed minimal differences. The data showed that temperature, humidity, UV intensity and wind direction did not seem to have noticeable effects on the NO reduction ability of the blocks. The details of weather conditions were obtained from the local observatory website which gave an approximation of the condition at site.

Figure 7.10 Sampling locations

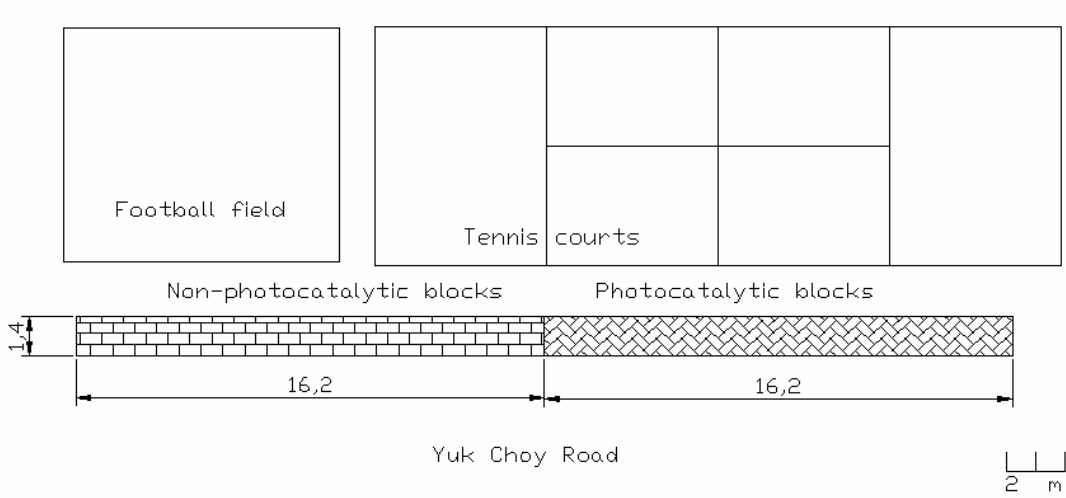


Figure 7.11 Collection of air bag at breathing zone



Table 7.4 Weather conditions for each measurement [HK Observatory, 2004]

Measurement	Weather condition					
	Temperature (°C)	Humidity (%)	UV intensity	Air pollution index		Wind direction
				General	Roadside	
M1	27	54	3	75-100	80-115	N
M2	24	93	3	65-90	80-100	NE
M3	23	76	3	60-70	70-100	N
M4	25	73	3	50-60	65-100	E
M5	24	70	3	55-70	70-105	E
M6	22	75	1	30-50	55-75	E
M7	19	63	2	30-50	50-75	NE
M8	22	68	1	55-70	70-100	E
M9	23	80	2	40-60	65-85	E

Table 7.5 Data from air monitoring (P: photocatalytic paving, N: non-photocatalytic paving)

Measurement	Pollutant concentration							
	At ground level				At breathing zone			
	NO (ppb)	NO ₂ (ppb)	CO (ppm)	SO ₂ (ppm)	NO (ppb)	NO ₂ (ppb)	CO (ppm)	SO ₂ (ppm)
M1-P	56.9	14.5	2.62	0.015	64.9	14.4	2.63	0.015
M1-N	56.2	14.4	2.56	0.014	69.2	17.8	2.64	0.014
M2-P	119.0	19.9	2.34	0.015	120.3	21.4	2.36	0.015
M2-N	119.4	20.8	2.33	0.015	121.3	21.5	2.42	0.014
M3-P	120.7	20.9	2.3	0.015	121.8	21.0	2.29	0.015
M3-N	126.5	21.8	2.29	0.015	131.2	21.8	2.3	0.014
M4-P	122.9	19.4	2.27	0.013	124.5	19.8	2.28	0.013
M4-N	126.7	20.1	2.37	0.013	127.2	20.8	2.51	0.014
M5-P	13.7	36.4	1.97	0.014	13.5	40.5	1.98	0.014
M5-N	27.8	33.6	1.98	0.014	9.8	4.2	0	0
M6-P	53.5	41.5	1.35	0.001	57.5	45.3	1.43	0.002
M6-N	60.6	41.9	1.4	0.002	60.1	40.8	1.39	0.002
M7-P	86.2	20.0	1.36	0.003	104.2	26.0	1.36	0.003
M7-N	115.0	20.0	1.35	0.003	129.2	25.2	1.35	0.002
M8-P	63.5	32.9	0.82	0.002	58.8	37.0	0.81	0.002
M8-N	67.9	33.8	0.77	0.001	74.5	34.6	0.8	0.003
M9-P	45.8	35.8	0.87	0.002	51.5	35.2	0.89	0.003
M9-N	48.1	36.4	0.87	0.002	52.8	36.1	0.91	0.002

Table 7.6 Percentage drop of pollutant concentration

Measurement	% drop of pollutant concentration due to photocatalytic paving							
	At ground level				At breathing zone			
	NO	NO ₂	CO	SO ₂	NO	NO ₂	CO	SO ₂
M1	-1	-1	-2	-7	6	19	0	-7
M2	0	4	0	0	1	1	2	-7
M3	5	4	0	0	7	4	0	-7
M4	3	3	4	0	2	5	9	7
M5	51	-8	1	0	10	4	0	0
M6	12	1	4	50	4	-11	-3	0
M7	25	0	0	0	19	-3	-1	-50
M8	6	3	-6	-100	21	-7	-1	33
M9	5	2	0	0	2	3	2	-50
Average	12%	1%	0%	-6%	8%	2%	1%	-1%

7.6 NO photodegradation after field trial

The durability of the paving blocks was analysed according to the ability of the paving blocks to remove NO after four months site usage as pavement. The four month period was restricted to the research period, and longer periods should also be monitored.

As shown in Table 7.7, the mean ability to remove NO was $2.17 \text{ mg hr}^{-1} \text{ m}^{-2}$ and $1.62 \text{ mg hr}^{-1} \text{ m}^{-2}$ for new blocks and for blocks after 4 month usage, respectively. A drop of 25 % was experienced after four months usage. Using another type of photocatalytic block, Yu [2003] reported that a mean drop in activity of 62 % was experienced after four months usage for a particular type of photocatalytic paving block which has been commercially available.

Yu [2003] indicated that the large open void texture of the commercially available product (Figure 7.12) resulted in a degradation in its pollutant removal ability due to dust and dirt being trapped in the pores after being used as paving. Hence it is anticipated that the performance of the air photocatalytic block presented in this study will not deteriorate as much due to its relatively dense surface texture (Figure 7.13).

Table 7.7 The activities of paving blocks

Mix notation	Mean NO removal of blocks ($\text{mghr}^{-1}\text{m}^{-2}$)
New paving blocks	2.17
Paving blocks after four months usage	1.62
Percentage drop after usage	25 %

Figure 7.12 Commercially available photocatalytic block



Figure 7.13 Self-designed photocatalytic block



CONCLUSIONS

8.1 Conclusions

This thesis has presented the findings of a research study on the design of an air pollutant removing paving block, which can make use of the local waste materials. Since C&DW, recycled glass and furnace bottom ash are readily available locally, this technology can be produced at a lower cost compared to other photocatalytic technologies available in the market. The design of the paving block can be made with as high as 80 % recycled material.

This study has focused on the factors which would affect the physical properties as well as the ability of removal of NO by the paving blocks. In order to derive a suitable mix design for the paving blocks the factors affecting NO photodegradation were investigated. The results indicated that porosity effectively increased the adsorption area available to pollutants, and hence the ability to remove NO was improved. The porosity of the paving blocks was affected by the type of materials with which they were prepared. Materials with a lower density led to a higher porosity of the blocks. The size of the materials used also affected the porosity of the paving blocks. Materials with less fine particles increased the porosity of the paving blocks. The change in the cement content of the mixes had an obvious relationship to the NO removal ability. Mixes prepared with a lower cement content

were more effective than ones that didn't in removing NO, as cement particles can easily fill up the pores. Specimens tested at different curing ages showed different abilities of NO removal. The results showed that photocatalytic activity decreased during the ageing of cement specimens. This finding was a result of the closing up of pores due to continuous hydration and carbonization. In addition, NO photodegradation was found to be affected by the relative humidity. Photocatalytic activity might decrease significantly when the relative humidity was increased.

The effect of incorporating recycled crushed glass cullet into the mix design of the paving blocks was also investigated. Although glass is a material of high density, the results showed that recycled glass used as aggregates in the paving blocks were more effective at removing NO. The increased performance of the paving blocks was believed to be due to the high light transmitting characteristic of the glass cullets. In addition it was found that the use of different coloured glasses in the mix design had little effect towards NO photodegradation, but better grading of the materials when glass was incorporated would benefit the ability to remove NO. Alkali silica reaction of the paving blocks, as a result of the use of glass, was eliminated by the addition of either Metakaolin or fly ash.

Furthermore, three different types of photocatalysts were studied. P-25 TiO₂ from Degussa Company was compared to an anatase and a rutile form of TiO₂ from Ke Xiang Company. P-25 showed the best photocatalytic ability. This result agrees with previous studies. The photocatalytic ability of the rutile form was very close to

P-25 whereas the anatase form performed not as well. The use of the rutile form instead of P-25 was particularly appealing in terms of cost. The glass cullets were further coated with the photocatalyst and this was found to improve the NO photodegradation of the blocks.

An optimum surface layer mix design from the test results was selected for blocks manufactured in a plant. The selection criteria included: the physical properties, the ability to remove NO, cost consideration and practicability. The cement to aggregate ratio was 1:3, with the aggregate proportion consisting of 50 % recycled glass and 50 % sand. P-25 TiO₂ and Metakaolin were added at 8 and 5 % by weight of cement, respectively. Results showed that the use of the photocatalytic blocks as pavement for an area of approximately 23 m² reduced NO concentrations by 12 and 8 % at the ground level and breathing zone, respectively. The paving blocks were tested after four months usage. As found, the photocatalytic activity of these used blocks have a reduction of only 25 % of ability in comparison with a similar product in the market which claimed having 62% reduction ability.

8.2 Recommendations

The followings are recommended for further study:

- The photocatalytic pavement has only been monitored for 6 months, hence should be monitored for a longer duration to observe if there is any further decrease in photocatalytic activity.

- The photocatalytic blocks should be also laid in a number of different environments for comparison, such as pavements with a high level of pedestrians or congested urban areas.
- The photocatalytic efficiency of the paving blocks should be analysed at different humidities, light intensities, residence times, pollutant concentrations, and temperatures, in order to analyze the suitability of the paving blocks when used in different countries.
- The high cold-water absorption should be eliminated by utilizing materials of low water absorption such as glass in the base layer of the paving block or by other possible methods.
- This study believed that larger TiO_2 particles removed NO more effectively compared to the smaller particles, which contradicts many previous studies. Hence a method to justify whether smaller TiO_2 particles in the paving block are not as easy to activate, due to the presence of other materials such as cement which covered the TiO_2 particles, needs to be sought.
- Particle grading was found to be an essential factor affecting NO photodegradation, hence it would be useful to investigate the optimum overall particle grading that allows the most efficient NO photodegradation.
- To derive a suitable method to quantify the amount of nitric acid generated as a result of NO removal and the possible effects of nitric acid towards the paving blocks.

REFERENCES

ANPO, A. and TAKEUCHI, M. The design and development of highly reactive titanium oxide photocatalysts operating under visible light irradiation. Journal of Catalysis. vol. 216, no. 1-2, pp. 505-516 (2003)

AO, C.H., LEE, S.C., MAK, C.L. and CHAN, L.Y. Photodegradation of volatile organic compounds (VOCs) and NO for indoor air purification using TiO₂: promotion versus inhibition effect of NO. Applied Catalysis B: Environmental. vol. 1294, pp. 1-11 (2002)

AOKI, S. The light clean revolution. Look Japan. Look Japan Limited (2002)

AQUINO, W., LANGE, D.A. and OLEK, J., The influence of metakaolin and silica fume on the chemistry of alkali-silica reaction products. Cement and Concrete Composites, vol. 23, no. 6, pp. 485-493 (2001)

AS/NZS 4456.14:2003 masonry units, segmental pavers and flags – method of test, method 14: determining water absorption properties. Standards Australia and Standards New Zealand (2003)

ASTM C150 REV A standard specification for portland cement. Annual Book of ASTM Standards (2004)

ASTM C618 standard specification for coal fly ash and raw or calcined natural pozzolan for use in concrete. Annual Book of ASTM Standards (2003a)

ASTM E303-93 (Reapproved 2003) standard test method for measuring surface frictional properties using the British pendulum tester. Annual Book of ASTM Standards (2003b)

ASTM C1260-01 standard test method for potential alkali reactivity of aggregates (mortar-bar method). Annual Book of ASTM Standards (2001)

BAROCH, P., MUSIL, J., VLCEK, J., NAM, K.H. and HAN, J.G. Reactive magnetron sputtering of TiO_x films. Surface and Coatings Technology. vol. 193, no. 1-3, pp. 107-111 (2004)

BS 6717 precast, unreinforced concrete paving blocks – requirements and test methods. British Standard Institution (2001)

BS 12 specification for portland cement. British Standard Institution (1996)

BS 6717-1 precast concrete paving blocks - part 1: specification for paving blocks. British Standard Institution (1993)

BS 812-103.1 testing aggregates – methods for determination of particle size distribution. British Standard Institution (1985)

Centamap. www.centamap.com. (2004)

CHAN A. T., HEDLEY A. J., HILLS P. R. and ZHONG J. H. The Air We Breathe: Air Pollution in Hong Kong. The University of Hong Kong, Hong Kong (2001)

CHAN, C. Y. H. and FONG, F. K. W. Development in Recycling of Construction and Demolition Materials. Government Printer, Hong Kong (2001)

CHEN H. J., YEN T. and CHEN K. H. Use of building rubbles as recycled aggregate. Cement and Concrete Research. vol. 3, pp. 125-132 (2003)

CHINI A. R., KUO S. S., ARMAGHANI J. M. and DUXBURY, J. P. Test of recycled concrete aggregate in accelerated test track. Journal of Transportation Engineering. vol. 127, no. 6, pp. 486 – 492 (2001)

CIVIC EXCHANGE. Hong Kong and Pearl River Delta Pilot Air Monitoring Project Executive Summary (2004a)

CIVIC EXCHANGE. Air Pollution – Air Quality Management Issues in The Hong Kong and The Pearl River Delta Region. Civic Exchange White Paper (2004b)

CIVIL ENGINEERING AND DEVELOPMENT DEPARTMENT (CEDD). Fill Management Division. Temporary Construction and Demolition Materials Recycling Facility in Tuen Mun Area 38 Fact Sheet (2004a)

CIVIL ENGINEERING AND DEVELOPMENT DEPARTMENT (CEDD). http://www.cedd.gov.hk/cgi_bin/cedd/TextOnly.pl?search=eng/services/recycling/index.htm. (2004b)

CIVIL ENGINEERING AND DEVELOPMENT DEPARTMENT (CEDD). Fill Management Division. Interim Review Report on Establishment of Pilot Construction and Demolition Material Recycling Facility in Tuen Mun Area 38. (2004c)

CIVIL ENGINEERING AND DEVELOPMENT DEPARTMENT (CEDD). Environmental Report 2003. Government Printer, Hong Kong (2003)

CIVIL ENGINEERING AND DEVELOPMENT DEPARTMENT (CEDD). Hong Kong Special Administrative Region Government General Specification for Civil Engineering Works. Hong Kong (1992)

COLLINS, R. J., HARRIS, D. J. and SPARKES, W. Blocks with Recycled Aggregate: Beam-and-Block Floors BRE Report IP 14/98. Building Research Establishment. United Kingdom (1998)

CUPERUS, J.C. and BOONE, J. International experiences in the use of recycled aggregates. In: DHIR R.K., NEWLANDS, M.D. and HALLIDAY, J.E. Proceedings of the International Symposium Recycling and Reuse of Waste Materials. Scotland (2003)

DALTON, J. S., JANES, P. A., JONES, N. G., NICHOLSON, J. A., HALLAM, K. R. and ALLEN, G. C. Photocatalytic oxidation of NO_x gases using TiO₂: a surface spectroscopic approach. Environmental Pollution. vol. 120, pp. 415-422 (2002)

DAWSON, A.R. Furnace bottom ash: its engineering properties and its use as a sub-base material. Proceedings of the Institution of Civil Engineers. pp. 993-1009 (1991)

DEHN, F., BAHNEMANN, D. and BILGER, B. Development of photocatalytically active coatings for concrete substrates. In: KASHINO, N. and OHAMA, Y. Proceedings of the RILEM International Symposium on Environment-Conscious Materials and Systems for Sustainable Development (2004)

DENG, X., YUE, Y. and GAO, Z. Gas-phase photo-oxidation of organic compounds over nanosized TiO₂ photocatalysts by various preparations. Applied Catalysis B: Environmental. vol. 39, pp. 135-147 (2002)

DEVAHASDIN, S., FAN JR., C., LI, K. and CHEN, D.H. TiO₂ Photocatalytic oxidation of nitric oxide: transient behaviour and reaction kinetics. Journal of Photochemistry and Photobiology A: Chemistry. vol. 156, pp. 161-170 (2003)

DHIR, R. K., LIMBACHIYA, M. C. and LEELAWAT, T. Suitability of recycled concrete aggregate for use in BS 5328 designated mixes. Structures and Buildings. vol. 134, pp. 257-274 (1999)

DIEBOLD, U. The surface science of titanium dioxide. Surface Science Reports. vol. 48, pp. 53-229 (2003)

DOMENECH, X. Photocatalysis for aqueous phase decontamination: is TiO₂ the better choice? In: OLLIS, D.F. and AL-EKABI H. Photocatalytic Purification and Treatment of Water and Air: Proceedings of the First International Conference on TiO₂ Photocatalytic Purification and Treatment of Water and Air (1992)

EL-SHEIKH, A.H., NEWMAN, A.P., AL-DAFFAEE, H., PHULL, S., CRESSWELL, N. and YORK, S. Deposition of anatase on the surface of activated carbon. Surface and Coatings Technology. vol. 187, pp. 284-292 (2004)

ENVIRONMENTAL COUNCIL OF CONCRETE ORGANISATIONS (ECCO).
Recycling Concrete and Masonry. Environmental Council of Concrete Organization
(1999)

ENVIRONMENTAL PROTECTION DEPARTMENT (EPD). Cleaning the air at
street level.
www.epd.gov.hk/epd/english/environmentinhk/air/prob_solutions/cleaning_air_atroad.html. (2005a)

ENVIRONMENTAL PROTECTION DEPARTMENT (EPD). An overview on air
quality and air pollution control in Hong Kong.
http://www.epd.gov.hk/epd/english/environmentinhk/air/air_maincontent.html.
(2005b)

ENVIRONMENTAL PROTECTION DEPARTMENT (EPD). Environment Hong
Kong 2004. Government Printer, Hong Kong (2004)

ENVIRONMENTAL PROTECTION DEPARTMENT (EPD). Monitoring of Solid
Waste in Hong Kong 2003. Government Printer, Hong Kong (2003a)

ENVIRONMENTAL PROTECTION DEPARTMENT (EPD). Air Quality in Hong Kong 2002. Government Printer, Hong Kong (2003b)

FONG, W.F.K. and YEUNG, J.S.K. “Production and application of recycled aggregates” in green buildings. Proceedings of One Day Seminar Organized by The Hong Kong Institution of Engineers. pp. 39-48 (2003)

FOX, M.A. and DULAY, M.T. Heterogeneous photocatalysis. Chemical Reviews. vol. 93, pp. 341-357 (1993)

FUJISHIMA, A., RAO, T. N. and TRYK, D. A. Titanium dioxide photocatalysis. Journal of Photochemistry and Photobiology C: Photochemistry Reviews 1. pp. 1-21 (2000)

FUJISHIMA, A., HASHIMOTO, K. and WATANABE, T. TiO₂ Photocatalysis Fundamentals and Applications. BKC, Japan (1999)

FUJISHIMA, A. and HONDA, K. Electrochemical photolysis of water at a semiconductor electrode. Nature. vol. 37, pp.238 (1972)

HOFFMANN, M.R., MARTIN, S.T., CHOI, W. and BAHNEMANN, D.W. Environmental applications of semiconductor photocatalysis. Chemical Review. vol. 95, pp. 69-96 (1995)

HONG KONG GOVERNMENT. Hong Kong Yearbook.

www.info.gov.hk/yearbook. (1997-2003)

HONG KONG OBSERVATORY. www.hko.gov.hk. (2004)

HONG KONG WETLAND PARK (HKWLP).

www.afcd.gov.hk/others/wetlandpark/html-en/master-aboutwetland.htm. (2004)

HUNG, W.T., CHEUNG, C.S. and KONG, H.A. Proceedings of the better air quality 2002. Regional Workshop on Better Air Quality in Asian Pacific Rim Cities. vol. 3 (2002)

JUNG, K.Y. and PARK, S.B. Photoactivity of $\text{SiO}_2/\text{TiO}_2$ and $\text{ZrO}_2/\text{TiO}_2$ mixed oxides prepared by sol-gel method. Materials Letters. vol. 58, pp. 2897-2900 (2004)

KAMIYA, K., MURATA, Y. and YAMADA, Y. Cement based hydraulic composition having NO_x purifying function. JP 10291849 (1998)

KAYABALI, K. and BULUS, G. The usability of bottom ash as an engineering material when amended with different matrices. Engineering Geology. vol. 56, pp. 293-303 (2000)

KHALOO, A.R. Properties of concrete using crushed clinker brick as coarse aggregate. ACI Materials Journal. vol. 91, no. 2, pp. 401-407 (1994)

KIRSCH, H. What is photocatalysis. In: SERPONE, N. and PELIZZETTI, E. Photocatalysis Fundamentals and Applications. Wiley (1989)

KOMAZAKI, Y., SHIMIZU, H. and TANKA, S. A new measurement method for nitrogen dioxides in the air using an annular diffusion scrubber coated with titanium dioxide. Atmospheric Environment. vol. 33, pp. 4363-4371 (1999)

LACKHOFF, M., PRIETO, X., NESTLE, N., DEHN, F. and NIESSNER, R. Photocatalytic activity of semiconductor modified cement – influence of semiconductor type and cement ageing. Applied Catalysis B: Environmental. vol. 1330, pp. 1-12 (2003)

LAM, G. C. K., LEUNG, D. Y. C., NIEWIADOMSKI, M., PAND, S. W., LEE, A. W. F. and LOUIE, P. K. K. Street level concentrations of nitrogen dioxide and suspended particulate matter in Hong Kong. Atmospheric Environment. vol. 33, pp. 1-11 (1999)

LINSEBIGLER, A.L., LU, G. and YATES JR., J.T. Photocatalysis on TiO₂ surfaces: principles, mechanisms and selected results. Chemical Review. vol. 95, pp. 735-758 (1995)

MANSUR, M.A., WEE, T.H. and CHERAN, L. S. Crushed bricks as coarse aggregate for concrete. ACI Materials Journal. vol. 96, no. 4, pp. 478-483 (1999)

mitsubishi materials corporation (mmc), www.mmc.co.jp (2005)

MURATA, Y., KAMITANI, K., TAWARA, H., OBATA, H. and YAMADA, Y. NO_x Removing Pavement Structure. US Patent Office. Patent No.6454489. (2002)

MURATA, Y., OBATA, H., TAWARA, H. and MURATA, K. NO Sub X-cleaning Paving Block. US Patent Office. Patent No.5861205 (1999a)

MURATA, Y., TAWARA H., OBATA, H. and TAKEUCHI, K. Air purifying pavement: development of photocatalytic concrete blocks. Journal of Advanced Oxidation Technology. vol. 4, no. 2, pp. 227-230 (1999b)

NATAATMADJA, A. and TAN, Y. L. Resilient response of recycled concrete road aggregates. Journal of Transportation Engineering. vol. 127, no. 5, pp. 450 – 453 (2001)

NONOYAMA, N and KOGA, H. Air Purification Functioning Road and Method for Purifying Polluted Air over Road. US Patent 6699577 (2000)

OBEE, T.N. and BROWN, R.T. TiO₂ photocatalysis for indoor air applications: effects of humidity and trace contaminant levels on the oxidation rates of formaldehyde, toluene and 1,3-butadiene. Environmental Science and Technology. vol. 29, pp. 1223-1231 (1995)

OHNO, T., SARUKAWA, K., TOKIEDA, K. and MATSUMURA, M. Morphology of a TiO₂ photocatalyst (Degussa P-25) consisting of anatase and rutile crystalline phases. Journal of Catalysis. vol. 203, pp. 82-86 (2001)

OKURA, I. and KANEKO, M. Photocatalysis Science and Technology. Springer, Berlin (2002)

OLORUNSOGO, F.T. Early age properties of recycled aggregate concrete. In: DHIR, R.K. and JAPPY, T.G. Proceedings of the International Conference on Exploiting Wastes in Concrete. Thomas Telford. pp. 165-170 (1999)

OPPENLANDER, T. Photochemical Purification of Water and Air. Wiley-vch, Germany (2003)

PALMGREN, F., BERKOWICZ, R., HERTEL, O. and VIGNATI, E. Effects of reduction of NO_x on the NO₂ levels in urban streets. The Science of the Total Environment. vol. 189/190, pp. 409-415 (1996)

PARK, T. Application of construction and building debris as base and sub-base materials in rigid pavement. Journal of Transportation Engineering. vol. 129, no. 5, pp. 558 – 563 (2003)

PARMON, V.N. Photocatalysis as a phenomenon: aspects of terminology. Catalysis Today. vol. 39, pp. 137-144 (1997)

POON, C.S. Trial Production and Performance Monitoring of Paving Blocks Made with Recycled Construction and Demolition Materials - Final report Prepared for the Civil Engineering Development Department of HKSAR. ECF 27/2001 (2004)

POON, C.S, KOU, S.C. and LAM, L. Building or Paving Blocks. Hong Kong Patent Office. Patent No. HK1043907. Hong Kong (2002)

POON, C.S., LAM, L., KOU, S.C., WONG, Y.L. and WONG, R. Rate of pozzolanic reaction of metakaolin in high-performance cement pastes. Cement and Concrete Research. vol. 31, pp. 1301-1306 (2001a)

POON, C.S., YU, A.T.W. and NG, L.H. On-site sorting of construction and demolition waste in Hong Kong. Resources Conservation and Recycling. vol. 32, pp. 157-172 (2001b)

PRATSINIS, S.E. Flame synthesis of nanosize particles: precise control of particle size. Journal of Aerosol Science. vol. 27, pp. 153-154 (1996)

RASHWAN, M. S., and ABOURIZK, S. The properties of recycled concrete. Concrete International. pp. 56-60 (1997)

ROBERTSON, P. K. J. Semiconductor photocatalysis: an environmentally acceptable alternative production technique and effluent treatment process. Journal of Cleaner Production. vol. 4, no. 3-4, pp. 203-212 (1996)

RYU, J. S. An experimental study on the effect of recycled aggregate on concrete properties. Magazine of Concrete Research. vol. 54, no. 1, pp. 7-12 (2002)

SAWYER, C. N., MC CARTY, P. Z. and PARKIN, G. F. Chemistry for Environmental Engineering and Science. Fifth Edition. Mc Graw-Hill, New York (2003)

SERPONE, N. Brief introductory remarks on heterogeneous photocatalysis. Solar Energy Materials and Solar Cells. vol. 38, pp. 369-379 (1995)

TAKASHI, I. and TAKEUCHI, K. Removal of low concentration nitrogen oxides through photoassisted heterogeneous catalysis. Journal of Molecular Catalysis. vol. 88, pp. 93-102 (1994)

TAVAKOLI, M. and SOROUSHIAN, P. Strengths of recycled aggregate concrete made using field demolished concrete as aggregate. ACI Materials Journal. vol. 93, no. 2, pp. 182-190 (1996)

TEXAS A&M UNIVERSITY. Wind-Borne Pollutants May Travel Thousands of Miles. Texas A&M University (2001)

THE NATIONAL INSTITUTE OF ADVANCED INDUSTRIAL SCIENCE AND TECHNOLOGY (NIAIST). Technical Report (Draft Proposal, Provisional Translation) – Testing Method for Air Purification Performance of Photocatalytic Material. NIAIST (2001)

TRYK, D.A., FUJISHIMA, A. and HONDA, K. Recent topics in photoelectrochemistry: achievements and future prospects. Electrochimica Acta. vol. 45, pp. 2363-2376 (2000)

WONG, A. Y. S. and TANNER, P. A. Monitoring environmental pollution in Hong Kong: trends and prospects. Trends in Analytical Chemistry. vol. 16, no.4, pp. 180-190 (1997)

WU, C., YUE, Y., DENG, X., HUA, W. and GAO, Z., Investigation on the synergetic effect between anatase and rutile nanoparticles in gas-phase photocatalytic oxidations. Catalysis Today. vol. 93, pp. 863-869 (2004)

YU, J.C.M. Deactivation and Regeneration of Environmentally Exposed Titanium Dioxide Based Products – Testing Report Prepared for the Environmental Protection Department. HKSAR E183413. Hong Kong (2003)

ZAKARIA, M. Strength and elasticity of brick and artificial aggregate concrete. Proceedings of the International Seminar on Exploiting Wastes in Concrete. United Kingdom (1999)

ZHANG, J., HU, Y., MATSUOKA, M., YAMASHITA, H., MINAGAWA, M., HIDAKA, H. and ANPO, M. Relationship between the local structures of titanium oxide photocatalysts and their reactivities in the decomposition of NO. The Journal of Physical Chemistry. vol. 105, no. 35, pp. 8395-8398 (2001)